PALACKY UNIVERSITY OLOMOUC

Faculty of Natural Sciences

Department of Biochemistry

The effect of graphene oxide on the pregnane X receptor signaling pathway regulating the biotransformation of xenobiotics

DIPLOMA THESIS

Author:	**Bc. Irena Malichová**
Study program:	B1406 Biochemie
Subject of study:	Biochemistry
Form of study:	Present
Supervisor:	**Mgr. Aneta Vrzalová, Ph.D.**
Year:	2017

I hereby declare, that I wrote the diploma thesis individually with mentioning all the references. I agree with making the thesis accessible according the law no. 111/1998 Sb., about the Universities, as subsequently amended. I got acquainted about the fact, that on my thesis apply the laws and duties based on law no. 121/2000 Sb., about author's law, as subsequently amended.

In Olomouc .....

Acknowledgements

I am very grateful to doc. Ing Radim Vrzal, Ph.D. for giving me the chance to work at Department of Cell Biology and Genetics at Palacky University. I thank very much to Mgr. Aneta Vrzalová, Ph.D. for excellent technical assistance, guidance and help during the experimental work. Further, I would like to thank for financial support from project IGA PrF-2016-003.

Bibliografická identifikace

Jméno a příjmení autora	Irena Malichová
Název práce	Vliv grafenoxidu na signalizaci pregnanového X receptoru regulujícího biotransformaci xenobiotik.
Typ práce	Magisterská
Pracoviště	Katedra buněčné biologie a genetiky
Vedoucí práce	Mgr. Aneta Vrzalová, Ph.D.
Rok obhajoby práce	2017

Abstrakt

Jelikož nanotechnologie přináší potenciál pro velké pokroky ve zdravotní péči, průmyslové sféře, a dokonce i v remediaci životního prostředí, zájem ohledně vývoje a využití nanomateriálů během posledních dvou desetiletí exponenciálně vzrostl. Díky své biokompatibilitě se velmi oblíbenými staly uhlíkové nanomateriály (uhlíkové a grafenové tečky) nacházející široké uplatnění v biomedicínských aplikacích. Jednou z nejnovějších senzací v této oblasti je dvoudimenzionální uhlíkový materiál známý jako grafen. Navzdory faktu, že výzkum zaměřený na technické a bio-medicinální využití grafenu a jeho derivátů se rozvíjí velmi rychle, pouze málo je známo o jejich interakci s biologickými systémy či toxicitě. Grafen oxid disponuje velkým měrným povrchem (2600 m^2/g), který mu propůjčuje vysokou kapacitu pro vazbu léčiv. Mimo jiné byla jako nežádoucí zjištěna zvýšená absorpce nepolárních kontaminantů životního prostředí u ryb, která vedla ke zvýšené indukci cytochromu P450 1A (cyp1A) zprostředkované aryluhlovodíkovým receptorem (AhR) ve srovnání s aktivátory AhR samotnými. Grafen oxid může tímto způsobem vykazovat účinky na další xenoreceptory, např. pregnanový X receptor (PXR), který je díky své široké substrátové specifitě k řadě cizorodých i tělu vlastních látek zodpovědný za kontrolu exprese mnoha genů zapojených do biotransformace léčiv. Cílem této práce je zjistit, zda grafen oxid ovlivňuje signalizaci pregnanového X receptoru (PXR) s následným dopadem na lidské zdraví skrz změnu exprese relevantních cílových genů, konkrétně *CYP3A4* a *MDR1*. Možné cyto-toxické působení grafen oxidu bylo studováno prostřednictvím MTT testu. Pomocí techniky gene reporter assay byla zkoumána schopnost PXR aktivovat promotor *CYP3A4* v přítomnosti GO. Poté s využitím metod qRT-PCR, a western blotting s imunodetekcí dle Sally Sue, byla sledována exprese u genů *CYP3A4* a *MDR1*, a to jak na úrovni mRNA, tak i na úrovni proteinů. Výsledky naznačují, že GO nanočástice ovlivňují signální dráhu jaderného pregnanového X receptoru, a to jak na úrovni transkripční (antagonistický mód), tak i na úrovni translační (agonistický i antagonistický mód). Přičemž efekt grafen oxidových nanočástic je závislý koncentraci těchto částic. Lze tedy předpokládat vznik možných lékových interakcí s dopadem na lidské zdraví.

Klíčová slova	Biotransformace, PXR, xenobiotika, grafen oxid
Počet stran	70
Počet příloh	0
Jazyk	Anglický

Bibliographical identification

Author's first name and surname	Irena Malichová
Title	The effect of graphene oxide on the pregnane X receptor signaling pathway regulating the biotransformation of xenobiotics.
Type of thesis	Master
Department	Department of Cell Biology and Genetics
Supervisor	Mgr. Aneta Vrzalová, Ph.D.
The year of presentation	2017

Abstract
Since nanotechnology holds out the promise of great improvements in healthcare, industrial technologies, and even in the remediation of the environment, the interest in exploration and application of nanomaterials has grown exponentially over the past two decades. Due to good biocompatibility, carbon nanomaterials (carbon and graphene dots) became very popular in broad spectrum of bio-medicinal applications. One of the latest sensations in the field of nanomaterials is a two-dimensional carbon material known as graphene. Despite the fact, that the research focused on technical and biomedical requests using graphene and its derivatives is expanding quickly, merely little is known about their interaction with the biological systems or internal toxicity. Graphene oxide owns large surface area (2600 m^2/g), which allows it to absorb drugs with remarkable capacity. However, undesirable GO-mediated higher cellular absorption of organic pollutants such as polycyclic aromatic hydrocarbons and polychlorinated biphenyls leading to increased induction of cytochrome P450 1A (cyp1A), mediated by aryl hydrocarbon receptor (AhR), was observed. To this end, we decided to investigate whether the graphene oxide may influence other nuclear receptors as well, specifically the pregnane X receptor (PXR) in humans. PXR is a promiscuous nuclear receptor that responds to a variety of endogenous and exogenous substances. Moreover, PXR plays a crucial role in a drug metabolism. We studied the potential hazardous effect of GO with the focus on the PXR-target genes, *CYP3A4* and *MDR1* respectively. Potential GO cytotoxicity was examined by MTT test. In addition, using a reporter gene assay, we monitored the ability of PXR to activate *CYP3A4* promoter in LS180 cell line during GO treatment. Moreover, employing methods like qRT-PCR, SDS-PAGE, western blotting and immunodetection using Sally Sue, we monitored the expressions of *CYP3A4* and *MDR1* genes at mRNA and protein levels. Our results indicate that graphene oxide nanoparticles dose-dependently influence the PXR signaling pathway, not only at the transcriptional level (antagonistic mode) but also at the translational level (agonistic and antagonistic mode), and therefore they may cause drug-drug interactions and have an impact on human health.

Keywords	Biotransformation, PXR, xenobiotics, graphene oxide
Number of pages	70
Number of appendices	0
Language	English

Goals

Theoretical part:

1) To summarize literature information about xenobiotics, biotransformation, cytochromes P450, pregnane X receptor and graphene-based nanomaterials.

Experimental part:

1) To investigate whether the graphene oxide have an influence on the viability of LS180 cells.
2) To investigate whether the graphene oxide influence the activation of pregnane X receptor.
3) To investigate whether the graphene oxide have an impact on the expression of PXR-driven genes at the mRNA level.
4) To investigate whether the graphene oxide have an impact on the expression of PXR-driven genes at the protein level.

1. Introduction

Organisms are constantly exposed to various exogenous compounds (xenobiotics). Xenobiotics may get into the inner system of organisms. Considering mammals, absorption takes place mostly via skin, lungs, or gastro-intestinal system. Absorbed substances are then spread out by bloodstream and reversibly distributed among the body tissues. To maintain the vital internal homeostasis, organisms evolved sophisticated systems for elimination of potentially toxic agents. Crucial element in homeostasis-maintenance is a biotransformation, i.e. a metabolism of xenobiotics. During the biotransformation, a chemical structure of xenobiotics is modified in order to increase the polarity and decrease the bioavailability of these compounds. This leads to water-soluble substances, which are easily eliminated from the body in urine, feces or sweat (Ferenčík *et al.*, 2000). Specific enzymes secure individual phases of xenobiotic metabolism, where cytochromes P450 are the major bio-catalysts involved in the first phase. Furthermore, in the II. phase various transferases are employed to secure conjugational reactions. Third phase of biotransformation includes the export of metabolites, with pharmacologically downregulated activity out of the cell.

Prominent regulatory elements of biotransformation enzymes are ligand-activated transcriptional factors so called nuclear receptors. Activated nuclear receptors bind to regulatory sequences of target genes and influence their expression. The object of interest in many toxicology-related studies is a pregnane X receptor (PXR). The PXR mediates a cellular response to vast range of exogenous compounds (Kliewer and Willson, 2002, Svecova *et al.*, 2008, Watkins *et al.*, 2001), where the most important target genes regulated by this receptor are *CYP3A* and xenobiotic efflux transporter multi-drug-resistant protein 1 (*MDR1).* Due to overlapping substrate specificity, PXR plays a significant role in mediating harmful drug-drug interactions in humans.

The signaling pathway of nuclear receptors might be compromised, potentially leading to life-threatening toxic effects. Over the past two decades the interest in nanomaterials has grown exponentially due to their enhanced or even unique properties. Graphene is one of the latest sensations in the field of nanomaterials. Naturally, its increasing production may lead to the release of graphene nano-sized sheets or nano-platelets into the environment. Despite the fact, that the research focused on

technical and biomedical requests of graphene and its derivatives is expanding quickly, merely little is known about their interaction with the biological systems or internal toxicity (Sanchez *et al.*, 2012). It was demonstrated that graphene oxide (GO) has remarkable capacity for absorbing organic pollutants such as polycyclic aromatic hydrocarbons and polychlorinated biphenyls (Karamani *et al.*, 2013). Furthermore, it was observed that GO increases the cellular absorption of organic pollutants in fish (Lammel and Navas, 2014). Therefore, we can speculate that in case of GO evasion, the hazard associated with an uptake of xenobiotics by organism might increase due to the ability of GO to bind these substances and releasing them intracellularly. Thus, it is a crucial task to obtain more information about possible threads, arising from the GO release into the environment and subsequent effects on the ecosystem health.

The aim of an experimental part of this study was to find out if the graphene oxide affects PXR signaling pathway, which might subsequently lead to disruption the PXR-dependent metabolism of xenobiotics with an impact on human health. Potential hazardous impact of GO was studied with focus on PXR-driven genes, *CYP3A4* and *MDR1*, respectively.

2. Present state of studied issues

2.1 Toxicology

Toxicology is a science focused on negative effects that occur in living organisms due to various chemicals. The environmental agents and chemical compounds found in nature, as well as pharmaceutical compounds that are synthesized for medical use may produce toxic effects in living organisms including disturbance in growth patterns, discomfort, disease, and death. The global goal of toxicology is to investigate the impact of these substances, especially xenobiotics, on the living organisms. The xenobiotic is a chemical substance which does not naturally occur within the organism. Toxicology outcomes provide the crucial information for an evaluation of safety and risks to the environment and living organisms after exposition to xenobiotics. With a focus on a particular aspect of toxicology, there are several branches of this scientific discipline. Toxicology subspecialties include: Clinical toxicology, Forensic toxicology, Environmental toxicology, Toxic-genomics, Regulatory toxicology, Chemical toxicology, Medical toxicology or Occupational toxicology.

Xenobiotics can be of natural or artificial origin. They are not a source of nutrients, on the other hand, they often produce physiological effects. They interfere with endogenous processes, which may lead to disruption of life-important homeostasis and endanger the life of the organism. In the past, the term ‘xenobiotics’ used to refer to poisonous substances. Nonetheless, the toxicity of a substance of any kind is always relative. It depends not only on the nature and dose of the substance itself, but also on individual organisms, their genetics or on a way how this particular agent is metabolized. Paracelsus said:’’ All things are poison and nothing is without poison, only the dose permits something not to be poisonous.’’ This so called ‘dose-response relationship’ is one of the major toxicology aspects. Nowadays, as a poison is considered a substance, causing a damage or death of the organism in small dose.

From early morning hygiene, through the breakfast, travel to work, to pills and cosmetics we use to make the ‘reality’ more bearable, during our daily routine we face endless amount of foreign substances. We simply cannot escape them, therefore, it is important to be aware of their possible side effects. The range of xenobiotics to which we are constantly exposed, is broad. Due to a diverse chemical structure, there are differences in their physical properties and physiological effects on specific organisms.

The biochemical and physiological effects of xenobiotics, and the mechanism of these effects, is studied by toxico-dynamics, whereas, toxico-kinetics is focused on the time-lapse movement of toxicants within the organism. Firstly, the xenobiotic must be absorbed, then it is distributed in the body, afterwards it is metabolized and finally the excretion takes place. This so-called ADME is a set of processes during the life of a xenobiotic within the organism.

2.2 Absorption, Distribution, and Elimination of toxic agents

Absorption means an entering of a substance into the body. The extent of absorption depends mainly on the lipophilicity and molecular weight of the substance. The body of mammals consists of several protective mechanisms and membrane barriers, which prevent the uptake and spreading of toxicants. Routes of administration are categorized by location, at which the substance is applied. Primary routes of administrations of xenobiotics are transdermal, gastrointestinal, and pulmonic. Classification of absorption might be also based on a location where the target of action is, such as topical, enteral, or parenteral.

Distribution is a process, when the absorbed compounds are carried via bloodstream to their effector sites, where they are reversibly exchanged between blood and tissues. Physical and chemical properties of the compound are of a capital importance for distribution. Most significant aspects, considering the physical-chemical properties, are molecular weight, lipophilicity, and acid dissociation constant pKa. These properties determine the transit of a substance through the cell membranes of tissue epithelium. Important elementary process, during the absorption and distribution of substances, is a transit through the physiological barriers. Transport mechanisms, providing the transit across the physiological barriers, are passive diffusion, facilitated diffusion, spread through the membrane pores, active transport, pinocytosis, endocytosis and exocytosis. With exception of passive diffusion, all transport mechanisms require specific membrane proteins. Lipophilic compounds with a small molecular weight are mostly transferred via passive diffusion. The flow direction in case of passive diffusion is from the side with a higher concentration of the substance towards the space with a lower concentration of the stated substance. This process doesn’t require ATP energy, because it uses the power of concentration gradient between these two regions. Low-molecular-weight substances such as water or urine can penetrate through the membrane thanks to membrane pores. Driving power, in this particular case, is osmosis or concentration gradient. More selective transport is secured by proteins called

transporters, which does not consummate ATP energy. This process is called facilitated diffusion. On the other hand, there are proteins like pumps or transporters which require ATP hydrolysis or other form of energy consumption. An example of active transporter is P-glycoprotein (ABCB1/MDR1) and other ABC transporters, participating on elimination of endogenous and exogenous substances. Common is the intake through an endocytosis, based on forming of a 'pouch', after a substance is recognized by specific receptor. This pouch, called endosome, may fuse with lysosomes leading to degradation of consumed substance or the endosome may transport its cargo to appointed destinations.

Elimination is a final process, when the xenobiotic leaves the body. During an evolution, the complexity of organisms increased. To protect themselves against the harsh outside world, organisms evolved physiological barriers. These barriers prevent absorption of possible toxicants, on the other hand, they also made the elimination process more difficult. This led to formation of sophisticated elimination systems. There are three main routes of elimination centralized in specific organs like kidneys, liver, and lungs. Polar compounds with molecular weight up to 65 kDa are primarily removed through the kidneys, leaving the body in urine. Liver provides enormous space for various biological processes, mostly here is enzymatically decreased the bioactivity and increased the polarity of xenobiotics with subsequent elimination into bile, then to gut leaving the body in feces. Volatile compounds can passively pervade through the membrane of alveolus, in lungs, and leave the body by exhaling. Other possible ways of excretion are minor, such as perspiration, salivation, or elimination into hair.

2.3 Drug metabolism (Biotransformation of xenobiotics)

Metabolism of xenobiotics also known as biotransformation, is a conversion of a compound to a metabolite. The term metabolite usually refers to small molecule of various functions. Biochemical reactions, which take place during the transformation of endogenous and exogenous substances, lead to excretion of these chemical compounds. Main goal of biotransformation is detoxification and lies in increasing the polarity of a substance via modifying the chemical structure and transforming the initial bioactive compound into pharmacologically inert one. It. Once the polarity is upregulated, the chemical compound becomes more water-soluble and leaves the body easily in urine, feces or sweat (Ferenčík *et al.*, 2000).

There are specific enzymes, with extensive substrate specificity, securing the biotransformation of wide range of xenobiotics. These enzymes are mainly located in liver and intestines, nevertheless they can be found in different organs like lungs, skin, breast, brain, etc. as well. After absorption and distribution, the xenobiotics are metabolized either in one or two phases.

2.3.1 Phase I

During the first phase of biotransformation the polarity of a substance is elevated. To make the substance more polar, several approaches are used in this phase. Firstly, a new functional group can be added, secondly a functional group can be removed, or thirdly a functional group can be transformed into more polar one. Compounds with high polarity might skip this phase and go straightly to phase II (Hodgson, 2012). Endogenous and exogenous substances undergo chemical reactions like oxidation (aromatic and aliphatic hydroxylation, de-alkylation, epoxidation, N-oxidation, de-halogenation), reductions, hydrolysis or hydrations (Skálová *et al.,* 2011). Eukaryotes prefer oxidation among other reactions. In general, cytochromes P450 (CYPs) are the major contributors to an oxidative xenobiotic metabolism. However, flavin monooxygenases (FMO) are also important in some cases of phase-I-metabolism and should not be overlooked.

Enzymes from FMO protein family can oxidize wide range of heteroatoms, especially soft nucleophiles like amines, phosphites and sulfides. For this reaction, an oxygen, NADPH and FAD are required. In mammals, five flavin monooxygenase genes were identified. The location, co-factor requirement and activity of FMO considering the xenobiotic metabolism were quite similar to the cytochrome P450 (Massey, 1994).

2.3.1.1 Cytochromes P450

Cytochromes P450 are hem-containing membrane proteins belonging to a superfamily traditionally assigned to hydroxylases, with mixed function of oxidases and monooxygenases. The term P450 originates from cytochromes identification process. It refers to the fact that reduced form of red pigment (P), bound with carbon monoxide, and absorbs light at 450 nm. CYPs are essential players in the maintenance of general human health, particularly as it relates to the metabolism of pharmaceuticals, and have superior role in oxidative biotransformation of many endogenous and foreign substances. It is estimated that CYP P450 are responsible for 80 % of xenobiotics metabolism during the phase I. Furthermore, cytochromes CYP P450 are involved in a spectrum of metabolic biosynthetic processes, such as biosynthesis of steroid hormones,

cholesterol, fat acids, bile acids and prostaglandins (Bernhardt, 2006). Some cytochromes P450 can also catalyze reactions essential to cell growth, development, ligand-modulated transcriptional regulation, neuroendocrine processes, and the induction of apoptosis.

All P450 enzymes exhibit similarity in their structure and general mechanism of action, nevertheless, in detailed look, there are differences in the function of specific enzymes as well as in the structures and qualities of active sites. Majority of CYPs substrates are hydrophobic (Graham-Lorence *et al.*, 1997). For CYP P450 to be catalytically active, an oxygen and reduction equivalents such as NADH or NADPH are required (Omura and Sato, 1964). The key function of CYP P450 is to initiate molecular oxygen to yield a reactive species that can attack moderately inert chemical sites, in order to introduce hydroxyl groups into the molecular constitution of these inert compounds. This enable the biotransformation of compounds that would otherwise lack functional groups fit for conjugation. Nevertheless, in addition to hydroxylation, cytochrome P450s can also catalyze a wide range of other chemical reactions including deamination, desulfuration, dehalogenations, epoxidations, N-, S-, and O-dealkylation, N-oxidations, peroxidation and sulfoxidation.

During the normal hydroxylation reaction catalyzed by cytochrome P450, molecular oxygen is split. One of the oxygen atoms is then incorporated into a target substrate molecule while the remaining oxygen atom is released as part of a water molecule (Fig. 1). The basic stoichiometry of a CYP P450-catalyzed hydroxylation reaction is represented by the following equation:

$$RH + NAD(P)H + O_2 + H^+ \rightarrow ROH + NAD(P)^+ + H_2O$$

CYPs P450, the enzymes with broad and overlapping substrate specificities, can be found from bacteria to humans. In mammals, most of these enzymes are located in the liver. However, a quite significant number of CYP P450 is also found in different tissues with higher exposure to xenobiotics, such as intestines or lungs. Each tissue has its own CYP P450 enzyme profile (Ding and Kaminsky, 2003). In general, eukaryotic cytochromes P450 are 480 to 560 amino acids long. Based on their subcellular localization, they can be divided into three groups. The two major groups of CYPs P450 in eukaryotes, are settled either on the cytosolic side of membrane of endoplasmic reticulum or on the membrane of mitochondria.

The CYPs in ER, are called as microsomal type and those situated in mitochondria are known as mitochondrial type. Third type of CYPs P450 in eukaryotes, is situated in cytosol.

Nowadays, 57 putatively functional genes encoding CYP P450 are known in humans while in mouse 108 functional genes have been identified (Nelson *et al.*, 1993, Nelson *et al.*, 2004). Human *CYP P450* genes are divided into 18 families and 43 subfamilies. Yet, the responsibility for most drug metabolism in humans and rats have three gene families *CYP1*, *CYP2* and *CYP3* (Wrighton *et al.*, 1996). To name and assign individual genes into families and subfamilies a standardized system of nomenclature was established. This system is based on the level of amino acid sequence identity, phylogenetic association and gene organization as determined by the P450 nomenclature Committee. The base for all cytochrome P450 genomic and cDNA sequence names is *CYP*. The Arabic numeral stand for individual family and the letter stands for subfamily. Member sequences within a subfamily are numbered successive as they are reported to the nomenclature committee. If P450 sequences display greater than 40 % amino acid identity they are placed in the same family. Similarly, those sequences that are over than 55 % identical are placed in the same subfamily. Those that are identical more than 97 %, are considered to represent alleles unless there is evidence to the contrary. According to these rules, the first officially-named cytochrome P450 was *CYP1A1* (Nebert and Nelson, 1991, Nelson *et al.*, 1993). For the mRNA and protein sequences the same nomenclature is used.

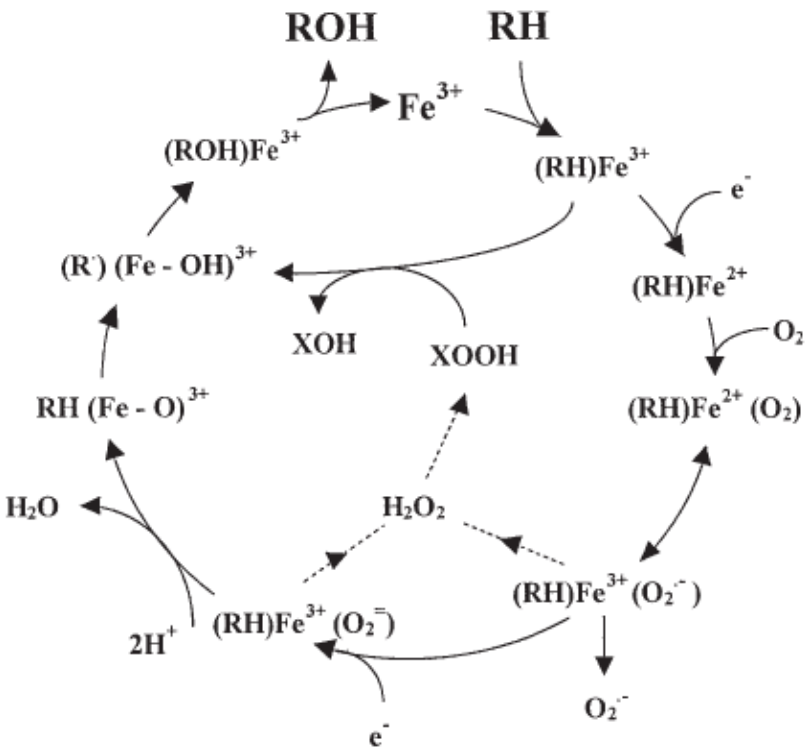

Fig. 1: Catalytic cycle of P450 enzymes. Adopted from (Anzenbacher and Anzenbacherova, 2001). R–H, substrate; R–OH, hydroxylated product; XOOH, peroxide (X = H or organic residue); XOH, hydroxylated by-product.

2.3.1.1.1 CYP3A subfamily

More than 50 % of administered drugs are metabolized by CYP3A subfamily (Fig. 2). In humans, CYP3 family includes only one subfamily, the CYP3A. This subfamily is located on chromosome 7q21 – 7q22.1 and has 231 kb in size. Four genes, namely *3A4*, *3A5, 3A7,* and *3A43* form CYP3A subfamily in humans. CYP3A enzymes can be induced by number of structurally unrelated compounds, like steroids, phenobarbitals, macrolide antibacterial and antifungal compounds. Expression of the three isoforms, CYP3A5, CYP3A7, and CYP3A43 is usually lower in comparison to CYP3A4 (Daly, 2006, Westlind-Johnsson *et al.*, 2003).

In humans, among the subfamily CYP3A, the most abundant and important enzyme is the CYP3A4. This enzyme was shown to be present in the liver, jejunum, colon, pancreas, and also in kidneys (Haehner *et al.*, 1996). CYP3A4 has a broad range of substrates, where most of these substrates are hydrophobic. The active site of CYP3A4 is large, flexible and can adapt to many favorably lipophilic compounds with relatively large structures and metabolize them (Hendrychova *et al.*, 2011, Scott and Halpert, 2005).

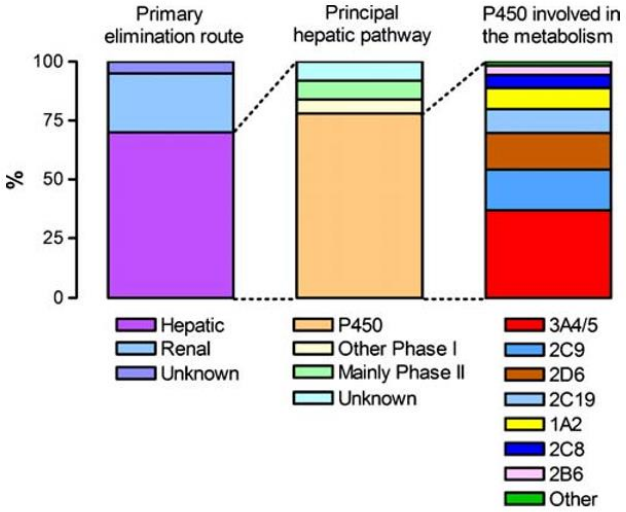

Fig. 2: The routes of elimination for the top 200 drugs by prescription in the United States according to the RxList data listed in April 2008 (http://www.rxlist.com). Adapted from (Wienkers and Heath, 2005)

Typical big substrates are immune-suppressants like cyclosporine A and tacrolimus, macrolide antibiotics like erythromycin, and anticancer drugs including taxol. Smaller molecules, including ifosfamide, tamoxifen, benzodiazepines, several statins, antidepressants, opioids are also recognized. CYP3A4 works also as an efficient steroid hydroxylase with an imperative role in the catabolism of several endogenous steroids, like testosterone, progesterone, androstenedione, cortisol and bile acids (Pelkonen *et al.*, 1998).

CYP3A4 can be induced by many agents, for example rifampicin, dexamethasone or phenobarbital via ligand-binding transcriptional factors also known as nuclear receptors (Smith and Jones, 1992). Intestinal and hepatic CYP3A4 enzymes are not coordinately regulated in their induction. The whole process of CYP3A induction on the molecular basis is not yet fully understood.

2.3.2 Phase II

The major process, linked with the second phase of xenobiotics metabolism, is a conjugation. Metabolites from the phase I merge with low-molecular-weight endogenous compounds. These reactions are catalyzed with specific conjugation enzymes, especially transferases. Most of these enzymes are situated in endoplasmic reticulum of hepatocytes. Reactions typical for phase II of biotransformation are glucoronidation, sulfonation, acetylation, methylation, conjugation with glutathione and

conjugation with amino acids (Skálová *et al.*, 2011). Thanks to these conjugational reactions, highly polar, hydrophilic, and less toxic compounds are made. Normally, the bioavailability of these intermediates is low and they are water-soluble, therefor they are more easily removed from the system than their parental compounds. On the other hand, even more toxic compounds might emerge during this process (Hodgson, 2012).

UDP-glukuronosyl transferases (UGTs) are enzymes responsible for metabolism of most endogenous and exogenous substances. UGT family consists of 116 members (Jancova *et al.*, 2010), and they are located in membranes. Formation of bond between nucleophilic atoms and uridin 5'-diphosphoglucoronic acid is secured by UGTs so-called glucoronidation (King *et al.*, 2000).

Sulfotransferases (SULTs) catalyze sulfonation, the conjugation with 3'phosphoadenosin 5'-phosphosulphate, so called PAPS, and nucleophilic acceptor group. Substrates for SULTs are for example steroids, catecholamine, eicosanoids, retinol, vitamin D, serotonin (Jancova *et al.*, 2010). Two classes of SULTs were found in mammals. SULTs that belong to the first class can be found on membrane of Golgi Apparatus and metabolize endogenous substances. The, second class of SULTs is localized in cytosol and participates on metabolism of xenobiotics and small endogenous molecules (Glatt *et al.*, 2001).

Glutathion-S-transferases (GSTs) are of main importance in detoxification of electrophilic substances and in protection against oxidative stress. In mammals, eight members of GST family were identified, which catalyze the conjugation of glutathione with xenobiotic (Sheehan *et al.*, 2001).

Acetyltransferases are mostly situated in the cytosol of enterocytes. These enzymes provide the transfer of acetyl from acetyl-Coenzyme A to free amino group in xenobiotic structure (Jancova *et al.*, 2010).

2.3.3 Phase III

Proteins which secure the transport of xenobiotics across the membrane, defined new- a third phase of biotransformation. Based on energy resource, transporters can be divide into three groups, primary, secondary, and tertiary, respectively. First to be discovered, and one of the most well-known primary transporter is P-glycoprotein (Juliano and Ling, 1976). Other transporters, providing the transport of varied compounds, are organic anion transporting polypeptides (OATPs) and organic cation transporters (OCTs) which are categorized as secondary transporters. OATPs generally transport

hydrophobic anoints, such as bile acids, thyroid hormones, organic color, or drugs, whereas, OCTs prefer hydrophilic compounds like choline, dopamine, histamine, adrenalin, etc. (Skálová *et al.*, 2011). Common goal of these transporters is to decrease the intracellular concentration of potentially toxic substances by the trans-epithelial efflux. However, this may lead to an undesirable effect in medical treatment, due to an insufficient drug concentration for its therapeutic effect (Schinkel and Jonker, 2003).

2.3.3.1 P-glycoprotein

P-glycoprotein (P-gp) belongs to a superfamily of ATP-binding cassette (ABC) transporters and is encoded by *ABCB1* gene. P-glycoprotein, also known as multidrug resistance protein (MDR1) or ATP-binding cassette subfamily B member 1 (ABCB1) or cluster of differentiation 243 (DC243), is an energy-dependent efflux transporter driven by ATP hydrolysis. In 1971, Juliano and Ling identified this transporter as a surface phospho-glycoprotein expressed in drug-resistant in cells from Chinese hamster ovary (Juliano and Ling, 1976).

P-glycoprotein is a 170 kDa transmembrane protein within 15 kDa glycosylation of N-terminal. This glycoprotein is composed of two homologous and symmetrical halves (cassettes). Each of these cassettes contains six transmembrane domains that are separated by an intracellular flexible linker polypeptide loop with an ATP-binding motif (Fig. 3). These ATP-binding domains of P-gp are located at the cytosolic side.

One of the most interesting aspects of P-glycoprotein is that a single integral membrane protein can recognize and transport various compounds, ranging from a molecular weight of 250 (cimetidine) to 1202 KDa (cyclosporine) (Pan *et al.*, 1994, Ueda *et al.*, 1997, Wu *et al.*, 1995). P-gp provides the efflux of immune-suppressives (cyclosporine A, tacrolimus), chemotherapeutics (Taxol, imatinib, doxorubicin), antibiotics (rifampicin, erythromycin), statins, or β-blockers as well as endogenous substrates like steroid hormones, cortisone, aldosterone, and hydrocortisone. Although, most substances transported by P-glycoprotein are alkaline or uncharged molecules, the only common sign is that majority of the P-glycoprotein substrates are hydrophobic. Important inhibitors of P-gp-dependent transport are cyclosporine A, valsporad (PSC833), verapamil, chinidin, Tween 80, amiodaron, tamoxifen, progesterone, ketoconazole, or a grapefruit juice (Skálová *et al.*, 2011).

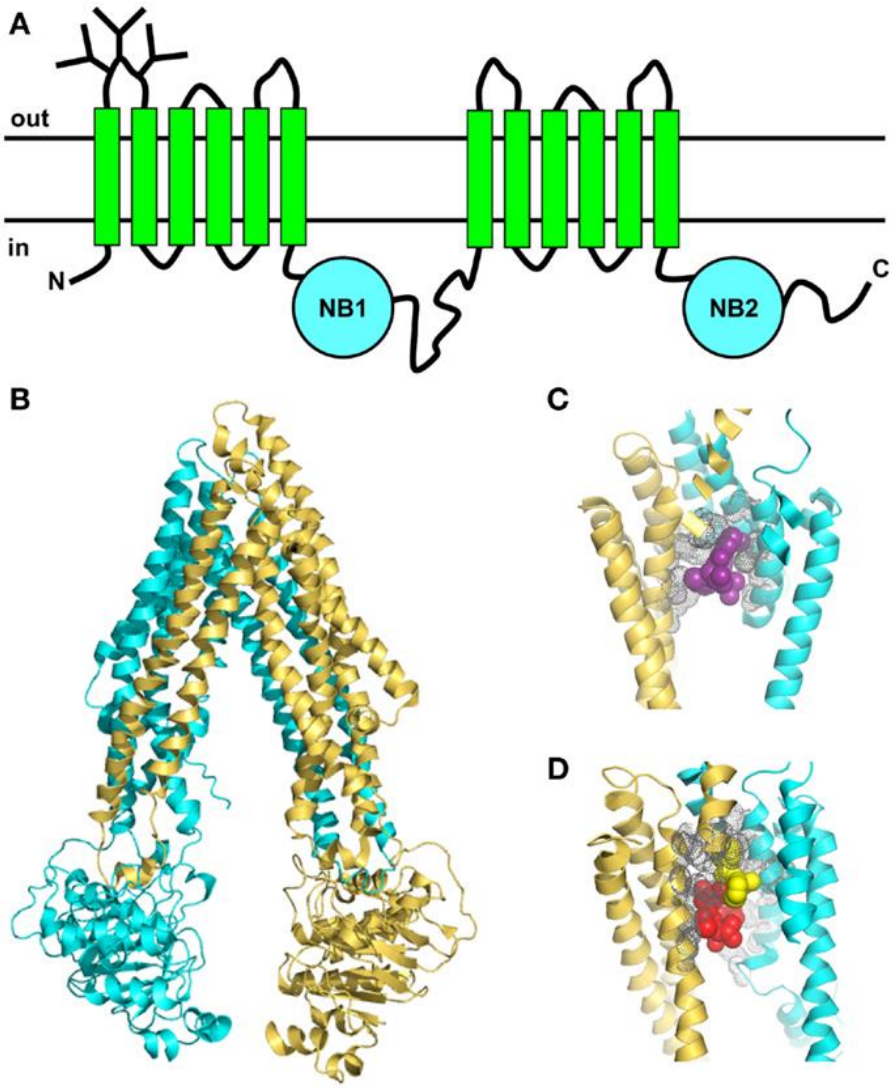

Fig. 3: Topology and X-ray crystal structure of P-gp. Adopted from (Sharom, 2014).
(A) The membrane topology shows two homologous halves, each with six TM segments and a NB domain on the cytoplasmic side, which binds and hydrolyzes ATP.
(B) X-ray crystal structure of mouse P-gp shows an inward-facing conformation in the absence of nucleotide (PDB 3G61).
(C, D) The drug-binding pocket of mouse P-gp as seen in the X-ray crystal structure.
(C) Close-up view (4.4 Å resolution) of one molecule of the cyclic peptide modulator QZ59-RRR (magenta, space-filling format) occupying the middle site inside the drug-binding pocket, with the volumes of nearby side-chains shown in gray (PDB 3G60).
(D) Close-up view of two molecules of the cyclic peptide modulator QZ59-SSS occupying the upper and lower sites (yellow and red, respectively, space-filling format) inside the drug-binding pocket, with the volumes of nearby side-chains shown in gray (PDB 3G61.

P-glycoprotein is expressed in normal tissues as well as in tumorous cells. In humans, two members of P-glycoprotein gene family (*MDR1*, *MDR3*) were identified, while in mice three members of this family (*mdr1a, mdr1b*, *mdr2*) were described (Gottesman and Pastan, 1993, Schinkel, 1997). Considering humans, P-gp can be found in the liver on the canaliculi surface of hepatocytes, in kidneys at the apical surface of

epithelial cells of proximal tubules, in the intestine in columnar epithelial cells, in the placental epithelial cells, and also in the brain on the luminal surface of capillary endothelial cells (Cordon-Cardo *et al.*, 1990, Thiebaut *et al.*, 1987). The distribution of intestinal P-glycoprotein is not even among the cells along the epithelial villi. Immuno-histological studies with human jejunum and colon using MRK16 antibody revealed, that high amounts of P-gp were observed only in the apical surface of the cells of columnar epithelium, but not in the crypt cells. Furthermore, the distribution of P-glycoprotein is not uniform along the length of intestine neither (Thiebaut *et al.*, 1987).

The anatomical localization of P-glycoprotein expression suggests that this efflux transporter can functionally protect the body against the toxic xenobiotics by elimination of these substances from hepatocytes, renal tubules and intestinal epithelial cells into the adjacent luminal space, leading to excretion of these compounds into bile, urine and the intestinal lumen, and preventing their accumulation in brain. Due to its localization, P-glycoprotein is believed to play a significant role in the processes of absorption, distribution, metabolism, and excretion of drugs in humans and animals (Ambudkar *et al.*, 1999, Gottesman and Pastan, 1993). Together with enzymes metabolizing the xenobiotics (especially CYP P450), the P-gp transporter forms an important protective mechanism against the toxic agents.

It was demonstrated, that P-gp is often overexpressed in cancer cells. Thus, traditional chemotherapy or a single therapeutic strategy often fails to achieve expected results in medical treatment due to multidrug resistance, mediated by drug efflux transporters such as P-gp. Moreover, the expression and function of P-gp are known to be easily and frequently modulated by P-gp substrates and/or cytochrome P450 CYP3A-related compounds, because of the strong overlapping substrate specificities between P-gp and CYP3A (Fromm, 2004, Greiner *et al.*, 1999). Among the population, the genetic polymorphisms have an impact on the amount of P-glycoprotein and its affinity to substrates, which might also represent a major source of individual variability in the potential toxicity and pharmacokinetics of drugs (Ambudkar *et al.*, 1999).

2.4 Regulation of biotransformation via nuclear receptors

Nuclear receptors (NR) are the prominent regulatory elements of a gene expression of enzymes participating in biotransformation. These receptors are activated by ligands, and act as transcriptional factors during the transcription of biotransformation enzymes (Fig. 4). Xenobiotics as well as endogenous substances may serve as their ligands. The cellular response to presence of ligands includes the activation of transcriptional cascades and expression of target genes. The gene expression of enzymes participating in drug metabolism is affected also by concentration of substrates, temperature, pH, and the presence of activators or inhibitors.

Activation of nuclear receptors commonly takes place in cytosol, where the receptors without ligands are usually situated. Members of NR1I family (PXR, CAR, VDR) show similarity in their structure, that includes the ligand-binding domain (LBD) at C-terminus of the receptor and the DNA-binding domain (DBD), situated at N-terminus of the receptor (Fig. 5). When a ligand bounds to LBD, it leads to conformational changes in protein structure and subsequent dissociation of corepressors like nuclear receptor corepressor (NCoR) and silencing mediator for retinoid and thyroid hormone receptor (SMRT).

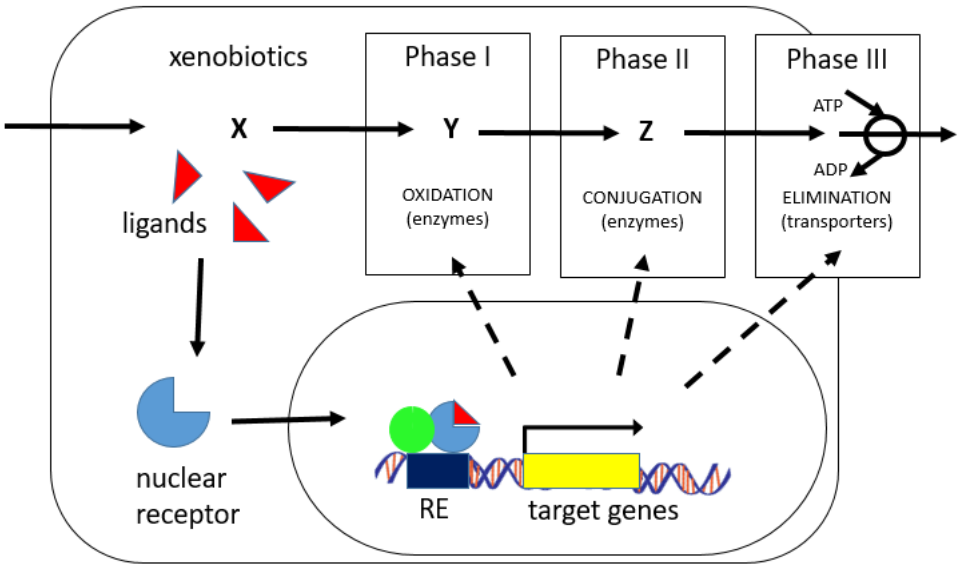

Fig. 4: Simplified scheme representing the regulation of phase I, II, and III of biotransformation. Based on figures presented by (Nakata *et al.*, 2006).
RE stands for a responsive element i.e. the DNA sequence where an activated nuclear receptor binds.

This allows the formation of heterodimer (mostly with RXR) and attachment of coactivators (e.g. SRC-1). Then the ligand-receptor complex is translocated into the nucleus, where the DBD interacts with specific DNA sequences known as responsive elements (REs) (Skálová *et al.*, 2011). Responsive elements are situated in regulatory regions of target genes. They consist of hexamer repetitions, which are arranged either directly in a row (DR), palindromatically inverted against each other (IR) or palindromatically everted from each other (ER).

Generally, an enzymatic inhibition of biotransformation enzymes is considered to be more relevant compared to an enzymatic induction. The reason is that it may lead to toxic effects because of possible increment of a xenobiotic concentration in blood. On the other hand, an induction of biotransformation enzymes, or transporters, decreases the level of drugs in blood system, which may lead to the loss of its therapeutic efficacy or loss of therapeutic efficacy of drugs used at the same time. Potential drug-drug interactions are of great importance in evaluation of xenobiotics for clinical use, especially during treatment of life-threatening diseases. Another, no less important issue when discussing induction of biotransformation enzymes, is a risk of resistance development in pathogens due to a decreased concentration of drugs under their therapeutic limits. Given to facts about serious possible negative consequences of drug-drug interactions, the induction and/or inhibition effects of xenobiotics should be carefully monitored parameters.

Two major groups are recognized in NRs, the receptors whose hormonal ligands have been identified- the nuclear hormone receptors (NHRs) and those whose ligands are unknown (or at least were unknown at the time of receptor identification)- the orphan receptors. Further the nuclear receptors could be divided into four categories (Mangelsdorf *et al.*, 1995). First, the receptors for steroid hormones functioning as homodimers. Second, the receptors that exist as heterodimers with RXR receptor and function in ligand-dependent manner. Third group includes orphan receptors functioning as homodimers binding to direct RE repeats, whereas fourth class consist of monomer orphan receptors binding to single site REs (Fig. 5).

Transcriptional regulation of gene expression of biotransformation enzymes is mainly secured by Aryl hydrocarbon Receptor (AhR), Constitutive Androstanol Receptor (CAR), Pregnane X Receptor (PXR), Vitamin D Receptor (VDR) and Glucocorticoid Receptor (GR). Beside these, there are other receptors like receptor for cis-retinal acid (RXR) and receptor for trans-retinal acid (RAR),

Fig. 5: Structural organization and classification of nuclear receptors. Adopted from (Olefsky, 2001).
At the top of the picture is shown the structure of NRs, where regions (A-F) are conserved in their function and sequence among NRs. A/B – N terminal domain, C – DNA-binding domain, D- hinge region, E- ligand-binding domain, F – C-terminal domain. Below are shown the four classes of NRs.

2.4.1 Aryl hydrocarbon Receptor

Aryl hydrocarbon receptor belongs to basic helix-loop-helix/Per-Arnt-Sim (bHLH-PAS) family of transcriptional factors (Tirona and Kim, 2005). AhR is expressed in most of organs and regulates biological response to many foreign substances (Vrzal *et al.*, 2004). AhR seems to play a role in development of many regulatory pathways, including hematopoiesis (Gasiewicz *et al.*, 2010), lymphoid systems (Kiss *et al.*, 2011, Li *et al.*, 2011) T-cells (Quintana *et al.*, 2008), neurons (Akahoshi *et al.*, 2006), and hepatocytes (Walisser *et al.*, 2005). AhR has also been found to have an important function in hematopoietic stem cells: AhR antagonism promotes their self-renewal and ex-vivo expansion (Boitano *et al.*, 2010) and is involved in megakaryocyte differentiation (Lindsey and Papoutsakis, 2011).

Xenobiotics that serve as AhR activators are for example polycyclic aromatic hydrocarbons (PAHs), polychlorinated biphenyls (PCBs) and dioxins. Activation of AhR receptor leads to higher expression of *CYP1A* and *CYP1B* genes, as well as to upregulated levels of UGT1A and GST enzymes (Mimura *et al.*, 1999, Nakata *et al.*, 2006). In absence of ligands, AhR is situated in cytosol in complex with two heat shock proteins hsp90, proteins XAP2 and p23. When a ligand binds to PAS B domain, change in 3D structure follows, which makes the nuclear-localization-signal (NLS) accessible and leads to nuclear import of this complex. In nucleus, hsp 90, XAP2 and p23 are removed and AhR-nuclear-translocator (ARNT) forms a heterodimer with AhR. ARNT/AhR heterodimer than binds to specific DNA sequences like xenobiotic-response-elements (XRE) or digoxin-response-element (DRE) and together with transcriptional coactivators, a transcription is initiated. These XRE/DRE elements contain specific sequences in promotor area of functional genes, which differ from those in responsive elements of NR1I family (Elbi *et al.*, 2002, Kewley *et al.*, 2004).

2.4.2 Constitutive Androstanol Receptor

In mammals, CAR positively regulates proteins involved in metabolism of drugs and steroids, while it suppresses the oxidation of fat acids and synthesis of glucose after phenobarbital-mediated induction (Ueda *et al.*, 2002). Unlike AhR, CAR is expressed in relatively small number of organs, in intestines and liver, respectively. There are two ways of CAR activation. First, a direct activation, secured by a ligand, which binds to CAR. In the second case, activators like phenobarbital or phenytoin activate CAR indirectly (without binding to CAR) via CAR phosphorylation by AMP-activated protein kinase. Both ways lead to gene expression of specific genes, such as *UGT1A1, CYP2B6, CYP3A4 a CYP2C9, SULT2A9, MRP3* a *OATP2* (Goodwin and Moore, 2004, Nakata *et al.*, 2006). As a close relative to PXR, the CAR evinces a cross-talk between PXR signaling pathway, which sometimes prevents a determining of a receptor responsible for induction of certain enzyme.

2.4.3 Receptor for Vitamin D

Receptor for vitamin D is mainly found in kidneys, intestine and bones (Dusso *et al.*, 2005). VDR participates on many physiological processes. VDR works as a major regulatory element in metabolism of calcium a phosphate in bones, it also plays role in immunity, cell growth a cell differentiation (Pospechova *et al.*, 2009).

2.4.4 Pregnane X Receptor

The pregnane X receptor (PXR), is a promiscuous nuclear receptor that responds to a variety of endogenous and exogenous substances. PXR was identified on the basis of its sequence homology with other nuclear receptors in expressed sequence tag (EST) databases. The receptor was named PXR based upon its activation by various natural and synthetic pregnanes (Kliewer *et al.*, 1998).

PXR belongs to the NR1I subfamily of nuclear receptors, this group consists of a mammalian vitamin D receptor (VDR; NR1I1) and constitutive androstanol receptor (CAR; NR1I3). PXR is highly expressed in the liver, small intestine, and colon, nonetheless low levels of PXR mRNA were detected also in kidneys, lungs, ovaries, stomach, or breast (Kodama and Negishi, 2013, Lehmann *et al.*, 1998). Notably, liver and intestines are the same tissues where *CYP3A* genes are most highly expressed and induced.

Elucidation of the 3D structure of the PXR ligand binding domain revealed that it has a large, spherical cavity that allows it to interact with various hydrophobic substances. Thus, unlike other nuclear receptors that interact selectively with specific ligands, PXR serves as a generalized sensor of hydrophobic substances. These substances usually bind to PXR with a low affinity (in micromoles). It was demonstrated, that PXR can be activated by xenobiotics such as antibiotics, antimycotics, and the herbal antidepressant St. John's wort, and also by endogenous compounds, including steroids and bile acids (Kliewer and Willson, 2002, Watkins *et al.*, 2001). Due to overlapping substrate specificity, PXR plays a significant role in mediating harmful drug-drug interactions in humans (Lehmann *et al.*, 1998).

Inactive form of PXR is located in cytosol in complex with chaperon protein Hsp90 and cytoplasmic CAR retention protein (CCRP). After a ligand binds to PXR, activated PXR is moved into nucleus, where a heterodimer with the 9-cis retinoid acid X receptor alpha, (RXRα, NR2B1) is made. This complex interacts with DNA PXR responsive element (PXRE) in the regulatory regions of target genes (Fig. 6). Characteristic repetitive sequence in PXRE is AG(G/T)CA arranged in direct (DR), invert (IR) or everted (ER) repeats. Heterodimer PXR-RXRα recognizes DR-3, ER-6, DR-4 and DR-5 motifs, where the numeral corresponds with number of nucleotides separating the individual repeats (Kliewer and Willson, 2002).

Activated PXR induces the gene expression of enzymes involved in all three phases of biotransformation (Albermann *et al.*, 2005, Maglich *et al.*, 2002). Further, it influences the metabolism of glucose, lipids, and bile acids (Nakamura *et al.*, 2007, Staudinger *et al.*, 2001). Most importantly, considering the metabolism of xenobiotics, the pregnane X receptor is the eminent regulator of the expression of the *CYP3A4* gene (Bertilsson *et al.*, 1998), which is said to be the most abundant drug-metabolizing enzyme in humans. PXR also regulates the expression of other genes involved in drug metabolism, including *CYP2C8, CYP2C9, CYP2B6*, *GSTA2* and genes encoding the transporters like *MDR1* and *MRP2* (Maglich *et al.*, 2002). It was proved that in upstream sequence of *MDR1* gene is present DR-4 motif recognized by PXR, and that activated PXR enhances the expression of *MDR1* also known as P-glycoprotein in human cell lines (Geick *et al.*, 2001, Synold *et al.*, 2001).

The extent of expression of PXR-driven genes significantly relies on the presence/absence of transcriptional regulators, coactivators, and corepressors. Steroid receptor coactivator 1 (SRC-1), hepatocyte nuclear factor 4α (HNF4α), peroxisome proliferator-activated receptor-γ coactivator-1α (PGC-1α), and binding protein p300 secure the activation of PXR-mediated transcription (Tirona *et al.*, 2003). On the contrary, inhibition of transcription arrives when corepressors like NCoR, SMRT a receptor interacting protein 140 (RIP140) are bound to specific DNA sequences (Tirona and Kim, 2005).

Besides the ligand-based modulation, and interactions with transcriptional regulators, the activity of nuclear receptors can be influenced via post-translational modifications (Smutny *et al.*, 2013) such as phosphorylation, ubiquitination, acetylation and SUMOylation, or via epigenetic regulation (Tian, 2013)

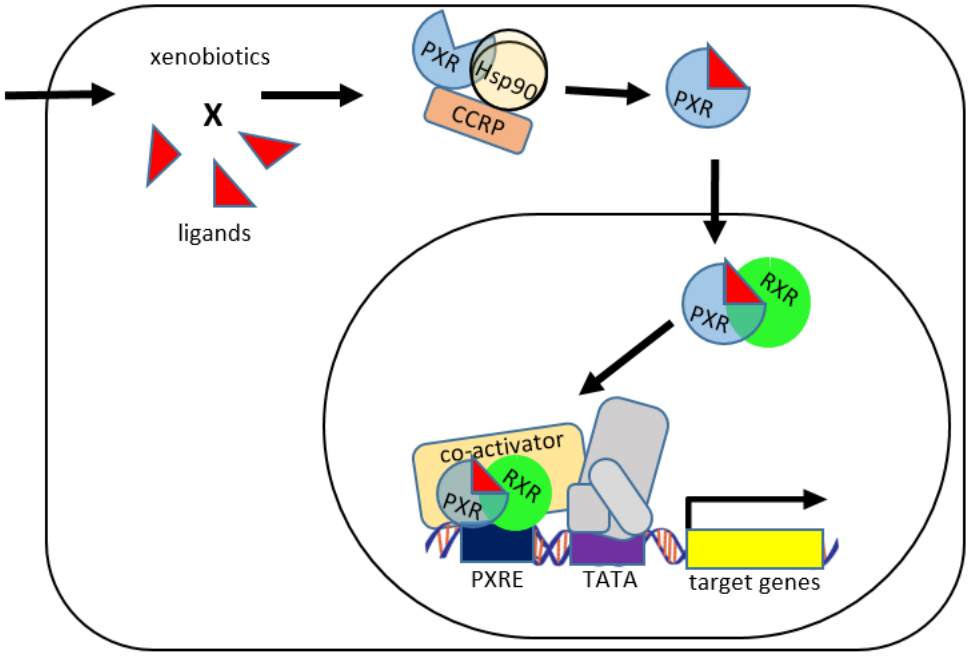

Fig. 6: Simplified scheme representing activation of pregnane X receptor. Based on figures presented by (Kodama and Negishi, 2013).

In vivo PXR exist as a phosphoprotein (Lichti-Kaiser *et al.*, 2009a). Using direct mutagenesis to alter the specific phosphorylation sites in the PXR structure, it was revealed that phosphorylation plays role in PXR activity, localization of PXR within the cell, ligand binding, RXRα-PXR heterodimer formation, as well as in interaction with PXRE and transcriptional cofactors (Lichti-Kaiser *et al.*, 2009a). Several kinases participate on regulation of PXR transcriptional activity, for example ribosomal p70 S6 kinase, cyclic AMP-dependent protein kinase A (PKA), Protein kinase C (PKC), Cyclin-dependent kinase 2 (Cdk2), and Cdk5 (Lichti-Kaiser *et al.*, 2009b, Pondugula *et al.*, 2009). In humans PKA signal cascade inhibits PXR-mediated gene expression, while opposing effect was observed in mice (Lichti-Kaiser *et al.*, 2009b). Further, PXR activity is regulated by mitogen-activated protein kinases (MAPKs). It was demonstrated that MAPK1 and MAPK2 negatively regulate the PXR signaling in HepG2 cell line (Smutny *et al.*, 2014).

Dominant site for acetylation of PXR was found to be on Lysin109. This posttranslational modification is secured by acetyltransferase p300 and leads to an inhibition of PXR-dependent transcriptional activity due to prevention of RXRα-PXR heterodimer formation (Pasquel *et al.*, 2016).

Ubiquitination leads to a degradation of PXR in proteasome, whereas small ubiquitin related modifiers (SUMOs), securing the conjugation/deconjugation processes, don't cause a protein degradation (Hu *et al.*, 2010a, Staudinger *et al.*, 2011). It was observed, that SUMOylation suppresses the rifampicin-dependent activation of PXR-driven gene expression, thus it is possible that SUMOs might influence biotransformation of xenobiotics (Tan *et al.*, 2016).

2.5 Nanomaterials

The world in 'nano' scale is highly promising; therefore, it is no surprise that in recent years, advances in nanotechnology along with the use of nanomaterials, strongly increased. According to British Standards Institution (2007), the American Society for Testing Materials (2006), and the Scientific Committee on Emerging and Newly-Identified Health Risks, a nanomaterial (NM) is a material with one dimension under 100 nm. Nanoparticles (NPs) are defined as materials with at least two dimensions between 1 to 100 nm. NPs can be of natural or anthropogenic origin. Before the term nanomaterials was defined, NPs found in the air were known as ultrafine particles and those found in soil or water as colloids (Lead *et al.*, 2006). In water systems, colloid is a general term applied to particles in the 1-nm to 1-xm size range. Aquatic colloids comprise organic macromolecular materials, such as fulvic and humic acids, proteins, peptides, as well as colloidal inorganic species, typically hydrous iron and manganese oxides. Their small size and huge surface area per unit mass makes them important binding phases for both, organic and inorganic contaminants. Also, a high surface energy, quantum confinement, and conformational behavior are likely to be important, although discussion of these parameters currently remains qualitative because of the complexity of colloids or NPs. However, the level of natural NPs is low (Klaine *et al.*, 2008, Roduner, 2006) . The effects of NPs on health of organisms are still being investigated, especially considering the humans. Nonetheless, the ecological systems were not paid such an attention.

Over the past two decades the interest in nanomaterials has grown exponentially. The reason is simple, NMs possess enhanced or even unique mechanical, catalytic, optical properties, and electrical conductivity primarily because of their nano-size. The development of new manufactured or engineered nanomaterials and their exploitation by burgeoning nanotechnology industries is a serious competition. Nowadays, the range of nanotechnology products is wide and can be divided into several compound classes,

including carbonaceous nanomaterials; metal oxides; semiconductor materials, including quantum dots; zero-valent metals such as iron, silver, and gold; and nano-polymers, such as dendrimers. Great number of products is being generated, including NPs as well as nanofibers, nanowires, and nano-sheets, and the range and types of NMs is continually expanding. Most of consumer product applications of NMs includes nanoparticle silver, for example wound dressings, socks, and other textiles; air filters; toothpaste; baby products; vacuum cleaners; and washing machines.

The higher use of these new materials brings uncertainty regarding the environmental impacts. It was demonstrated, that NPs can enter cells by diffusing through cell membranes as well as through endocytosis (Kim *et al.*, 2006) or adhesion (Geiser *et al.*, 2005). Some NMs, like quantum dots and CNTs, are designed to interact with proteins, nucleic acids, or cell membranes for labeling or drug delivery purposes (Gao *et al.*, 2002, Medintz *et al.*, 2005). The toxicity mechanisms haven't been completely elucidated for majority of NMs. Possible negative effects include disruption of membranes or membrane potential, oxidation of proteins, genotoxicity, interruption of energy transduction, or formation of reactive oxygen species.

Nanomaterial-protein interactions have been optimized for numerous biomedical applications. For example, quantum dots are used to target and fluorescently label proteins for imaging (Jaiswal *et al.*, 2004, Jaiswal *et al.*, 2003). Multi-walled CNTs were used in bio-sensing applications to immobilize and optimize lactate dehydrogenase and alcohol dehydrogenase (Tsai and Huang, 2007, Tsai *et al.*, 2007). In medical therapeutics, many drug candidates fail in reaching their targets at sufficient concentrations, which limit their effectiveness. However, when the drugs are encapsulated into nanoparticles and prevented from clumping, due to a large surface to volume ratio, the result is often a stable and water-soluble material (Brigger *et al.*, 2002, Panyam and Labhasetwar, 2003). New treatments, based on nanoparticle-mediated delivery systems, are being developed, like the preventive treatment of the oxidative damage occurring in neurodegenerative diseases like Alzheimer's, Wilson's and Parkinson's (Cui *et al.*, 2005, Dobson, 2001). It is obvious that nanotechnology holds out the promise of great improvements in economic growth, health, industrial technologies; and even in remediation of the environment.

2.5.1 Graphene

Graphene is one of the latest sensations in the field of nanomaterials. This two-dimensional material constitutes of layers of carbon atoms arranged in six-membered rings (Fig. 7a). It is distinctly different from carbon nanotubes and fullerenes (Fig. 7), and exhibits unique properties which fascinate the scientific community. In ideal case, graphene is a single-layer material, although graphene with two or more layers is being investigated with equal interest. There are three different types of graphene: single-layer graphene (SG), bilayer graphene (BG), and few-layer graphene (FG, number of layers <10) (Geim and Novoselov, 2007).

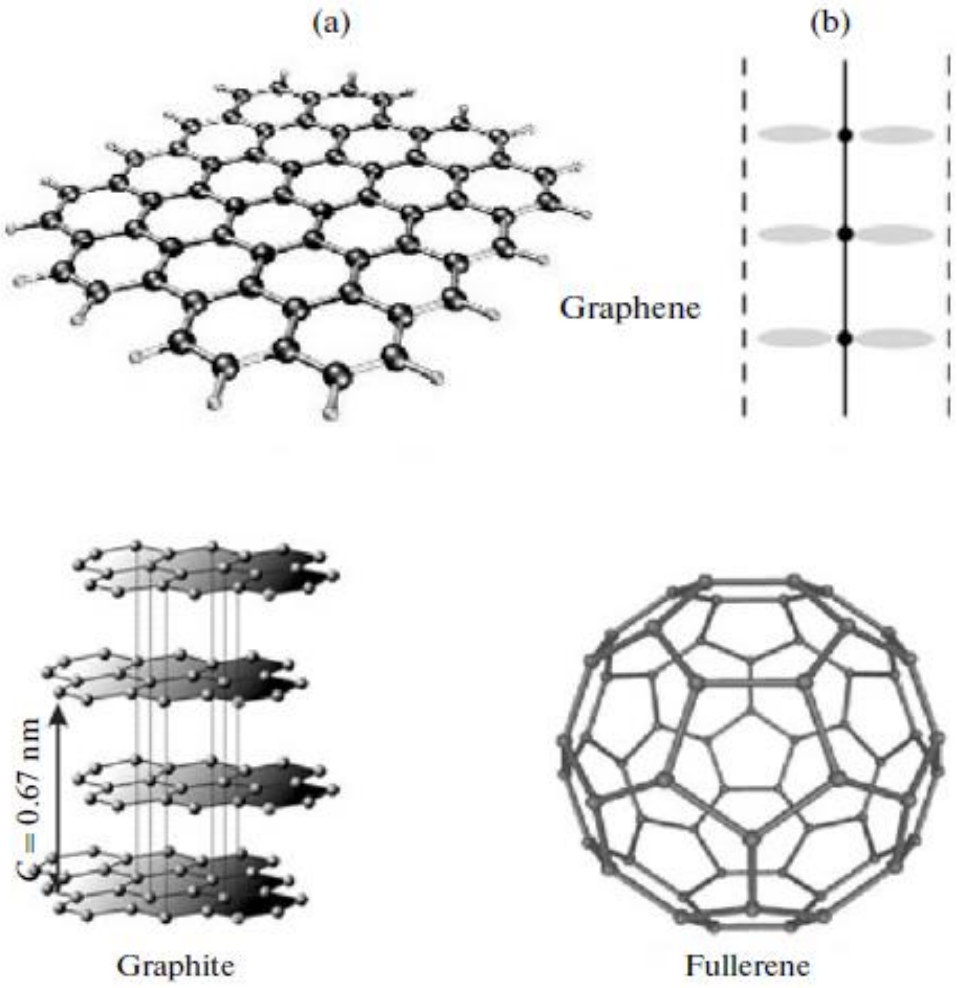

Fig. 7: Structure of graphene: (a) top view, (b) side view of the π_electron system. Also shown are the structure of a graphite crystal and a fullerene molecule. Adopted from (Tkachev *et al.*, 2011)

The single-layer graphene is usually prepared by micromechanical cleavage in which a highly oriented pyrolytic graphite (HOPG) is pealed with scotch-tape and deposited on to a silicon substrate. Other important methods employed in production of graphene samples are epitaxial growth on an insulator surface (such as SiC), chemical vapor deposition on the surface of single metal crystals (e.g., Ni), arc discharge of graphite under suitable conditions (Park and Ruoff, 2009). For example, a single-layer graphene was grown on top of a 6H-SiC substrate by an *ex situ* method, which gives larger mono-layer graphene, compared to in situ method (Emtsev *et al.*, 2009). Further, a high-quality graphene sheets of one to three layers were prepared on stainless steel substrates. The required conditions were 5008°C, secured by microwave plasma chemical vapor deposition in an atmosphere of 10% methane and 90% hydrogen at a pressure of 30 torr and a flow rate of 200 sccm (standard cubic centimeter per minute). Arc-discharge of graphite in hydrogen appears to yield primarily two- and three-layer graphene. Starting with graphite and using chemical exfoliation, a high-quality graphene with a predetermined number of layers can be obtained (Wu *et al.*, 2009).

Typical graphene properties are a quantum Hall effect at room temperature (Novoselov *et al.*, 2007), an ambipolar electric field effect along with ballistic conduction of charge carriers and high elasticity (Lee *et al.*, 2008). Although, the graphene should be perfectly flat, ripples occur because of thermal fluctuations (Novoselov *et al.*, 2007). A controversy surrounds magnetism in graphene because of possible contamination with magnetic impurities. Paramagnetic and certain other magnetic features including spin-glass behavior and magnetic switching phenomena have been observed in nano-graphite particles. Magnetic properties of nano-graphite or nano-graphene were reviewed by (Enoki and Takai, 2008). The crucial message is that the edge states, of adsorbed or intercalated species, play a significant role in determining the magnetic properties. In graphene ribbons, the edges play a crucial role in determining the electronic structure; the zigzag edges with nonbonding-electrons give a rise to the edge states (Nakada *et al.*, 1996, Ritter and Lyding, 2009).

In the temperature range 100 to 300 K, a few-layer graphene and also nano-graphite particles, show semiconducting or insulating behavior with their resistance. If the graphene is heated to high temperatures, the resistivity decreases, while the temperatures below 50 K cause an increase in the resistivity. Thus, graphene nano-ribbons acquired from exfoliation of graphite show semiconducting properties. It is outstanding that field-effect-transistor properties are present even though the samples

are defected. Even though, the graphene is not superconducting by itself, when it is positioned between superconducting electrodes it shows supercurrents over short distances due to the Josephson effect. A superconducting transistor based on graphene was prepared (Heersche *et al.*, 2007).

Significant work on graphene-polymer composites, about processing of nano-graphene platelets to produce composites (Kuilla *et al.*, 2010) indicates how a combination of adhesives and high-strength structures such as graphene and carbon nanotubes can yield strong, lightweight, and damage-resistant materials. Plenty of graphene properties are still not fully understood. Some possible applications of graphene are sensors, transistors, solar cells, targeted drug delivery, etc...

The toxicological aspects of diverse graphene samples need to be examined. Modified graphene (e.g., graphene in which carbon atoms are replaced extensively by boron or silicon atoms) as well as inorganic graphene constituted by layered materials, such as MoS_2, are likely to be rich areas for investigation. The increasing production of carbon NPs, due to its great potential for a broad range of industrial and consumer applications, may lead to release of graphene nano-sized sheets or nano-platelets into the environment. Possible interaction of NPs with organic contaminants might increase their toxicity and also influence the hazard associated with NPs uptake by organism. Thus, it is a crucial task to obtain more information about possible threads, arisen from the presence of graphene, or other NPs, in environment.

2.5.2 Graphene oxide

On the basal plane of graphene oxide (GO) are present epoxy groups, one or two ethers and tertiary hydroxyl groups, while at the edges of the sheet, lactones, ketones, carboxylic acid and ester groups can be found (Fig. 8) (Gao *et al.*, 2009). It was demonstrated, that oxidized graphene NMs are able serve as effective carrier systems for the targeted delivery of chemical compounds (Yang *et al.*, 2011, Zhu *et al.*, 2012) and biomolecules like proteins, DNA and siRNA (Bao *et al.*, 2011, Feng *et al.*, 2011). For example, a novel multifunctional GO with charge-reversal polyelectrolyte and integrin was synthetized and proved to be highly specific and efficient of controlled target delivery of doxorubicin in cancer treatment (Zhou *et al.*, 2014). Further, it was demonstrated that graphene oxide could serve for the delivery of bone morphogenetic protein-2 and substance P, and that this delivery promoted bone formation on titanium implants that were coated with GO (La *et al.*, 2014). Moreover, the potential of GO for

bio-sensing (Artiles *et al.*, 2011, Kuila *et al.*, 2011) and bio-imaging applications is being studied (Shen *et al.*, 2012, Zhang *et al.*, 2012, Zhu *et al.*, 2011). The materials, made of graphene or GO, showed to enhance the efficiency of implants and tissue engineered scaffolds (Lee *et al.*, 2011, Nayak *et al.*, 2011). Moreover, functionalized graphene oxide as a carrier for Adriamycin along with miR-21 targeted siRNA, showed potential to overcome tumor multidrug resistance, subsequently leading to enhancement of therapeutic efficacy (Zhi *et al.*, 2013).

Despite the fact, that the research, focused on the technical and biomedical requests of graphene and graphene-derived nanomaterials, is expanding quickly, pretty little is known about their interaction with the biological systems or internal toxicity (Sanchez *et al.*, 2012). Mechanisms that were proposed to underlie the cytotoxic effect (Fig. 9) include plasma membrane damage, deterioration of mitochondrial activity (Akhavan and Ghaderi, 2010, Sasidharan *et al.*, 2011, Zhang *et al.*, 2010), initiation of oxidative stress (Chang *et al.*, 2011, Yue *et al.*, 2012) and DNA damage (Akhavan *et al.*, 2012) ultimately leading to apoptotic and/or necrotic cell death0 (Li *et al.*, 2012, Yuan *et al.*, 2012).

Nevertheless, in some cases results obtained by different authors regarding the cytotoxicity of graphene-based NMs, are in contrary (particularly for GO). These inconsistencies might lie in different intrinsic properties of used NMs. The accessibility of the NMs during bioassays or the sensitivity of the used cell lines might be few of many factors resulting in different data. Additionally, considering the enormously high specific surface area of graphene NMs and their chemical temperament, like conjugated π-electron system, presence of reactive functional surface groups, they might interfere with some of the frequently used bioassays.

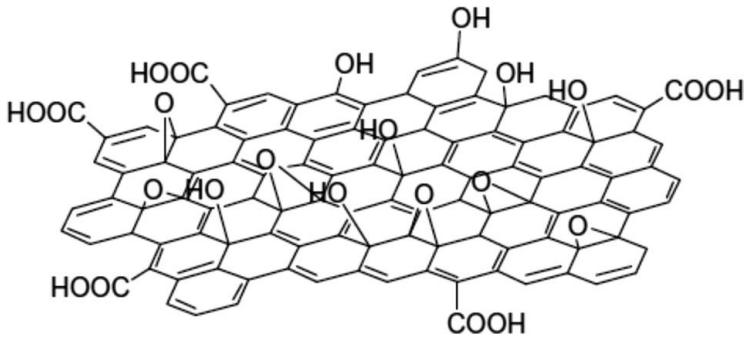

Fig. 8: Structure of graphene oxide. Adopted from (Nasrollahzadeh *et al.*, 2015)

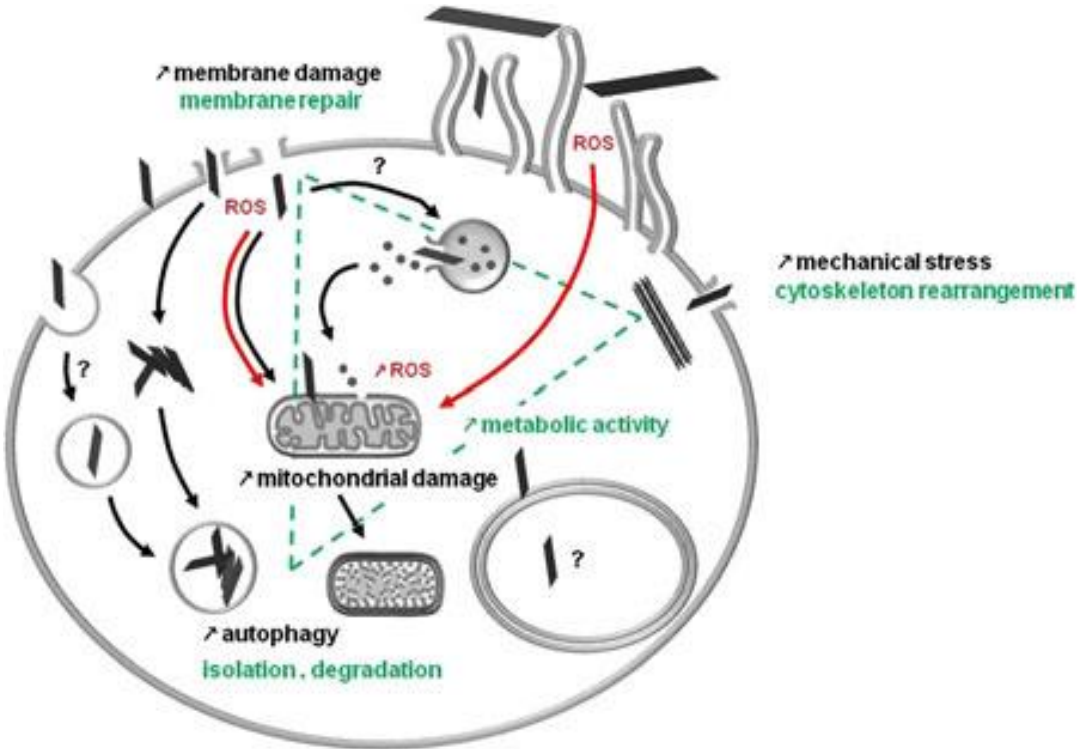

Fig. 9: Hypothetic model of graphene nanomaterial internalization and cytotoxicity. Adopted from (Lammel *et al.*, 2013).
Graphene oxide (GO) and carboxyl graphene (CXYG) nano-platelets penetrate through the plasma membrane into the cytosol, are concentrated and encapsulated in intracellular vesicles. Cells respond with the formation of cytokeratin filament bundles to mechanically reinforce the plasma membrane and initiate plasma membrane repair mechanisms. These processes involve an increase in metabolic activity. Exposure to GO and CXYG nano-platelets results in elevated intracellular ROS levels, perturbation of mitochondrial structure and function, and an augmented number of autophagosomes.

As mentioned above, some graphene derivatives, GO and carboxyl graphene (CXYG), are being studied for their possible use in technical and biomedical applications, therefor an accidental or intentional exposure may appear. An induction of oxidative stress is considered to be one of the major mechanisms underlying the cytotoxicity caused by nanomaterials (Pulskamp *et al.*, 2007, Shvedova *et al.*, 2012, Xia *et al.*, 2006). The cytotoxic effects of graphene might differ than those of other graphitic materials as cytotoxicity studies on graphene are far and few so far. It was observed, that GO and CXYG nano-platelets induce the production of intracellular ROS in a concentration and time-dependent manner. In addition, GO and CXYG-induced ROS formation seemed to follow different kinetics. For GO, top ROS levels were reached after exposure to 16 μg/ml for 24 h. In cells treated with lower GO concentrations (1 – 8 μg/ml) intracellular ROS levels were gradually increasing in the lapse between 24 and 72 h and finally reached levels comparable to those measured at 16 μg/ml (Lammel *et al.*, 2013).

It was shown that GO, have remarkable capacity of absorbing organic pollutants such as polycyclic aromatic hydrocarbons and polychlorinated biphenyls (Karamani *et al.*, 2013). Further, it was observed that GO in combination with AhR agonists, leads to higher induction of CYP1A mediated via AhR in fish, suggesting that GO can endanger the water organisms by increasing the cellular absorption of organic pollutants due its ability to bind these substances and releasing them intracellularly (Lammel and Navas, 2014). Considering the possible evasion of GO nano-platelets and the ability of GO to interact with organic compounds, it raises certain concerns about impact on environmental health.

3. Material and methods

3.1 Material

3.1.1 Chemicals

Tab. 1: List of used chemicals.

Methods	Chemicals	Manufacturer
Cultivation	Dublecco´s modified Eagle´s medium (4,5 g/l glucose; DMEM) Fetal Bovine Serum (FBS) Charcoal Stripped Fetal Bovine Serum (CS FBS) Non-essential Amino Acids L-glutamin 0,25 % Trypsin - EDTA Solution (T4049) Trypan blue (T6146)	Sigma-Aldrich, USA
	Phosphate-Buffered Saline (pH = 7,4; PBS)	Gibco, USA
Treatment	Rifampicin (RIF) Triton X-100 Dimethyl Sulfoxide (DMSO)	Sigma-Aldrich, USA
	Graphene oxide dispersion in water (2 mg/ml; GO)	Biotool.com, Germany
MTT test	3-(4,5-dimethylthiazol-2-yl)-2,5-diphenyltetrazolium bromide (MTT)	Sigma-Aldrich, USA
	Dimethyl Sulfoxide (DMSO)	Lach-Ner s.r.o., CZ
Reporter Gene Assay (RGA)	FuGENE® HD transfection reagent Reporter Plasmid (pGL4.10) Reporter Lysis 5x Buffer	Promega, USA
	Expression plasmid for human PXR (pSG5-hPXR)	Texas University, Dallas, Texas, USA
	Luciferase Substrate	-prepared-
RNA isolation	TRI Reagent (T9424) Chloroform RNase free water	Sigma-Aldrich, USA
	Isopropanol (20037-AT0) Ethanol (75 %)	Lach-Ner s.r.o., CZ
cDNA synthesis	Random Primers (N2201FA, 100 pm/µl) dNTP 10 mmol (dCTP, dTTP, dCTP, dATP)	TaKaRa, Japan
	RNase inhibitor Reverse Transcriptase M-MuLV (200000 U/ml) 10x reaction buffer (B0253S)	Biolabs, UK

Tab. 1: List of used chemicals (continuation).

Methods	Chemicals	Manufacturer
qRT - PCR	Probe Master UPL probe for CYP3A4 (number 38; 144035) UPL probe for GAPDH (number 60; 105132) UPL Probe for PgP (number 147; 101705)	Roche Diagnostic Corporation, Switzerland
	Primers for CYP3A4 (0,1 mmol; R: 836P6, F 836P5) Primers for GAPDH (0,1 mmol; R: 836P8, F: 836P7) Primers for MDR1 (0,1 mmol; R1064U5, F:1064U4)	Generi Biotech, CZ
Protein isolation	Lysis buffer for protein isolation (pH = 7,5)	-prepared-
	HEPES (H3375) EDTA (T9884-62)	Sigma-Aldrich, USA
	NaCl (02150)	Lach-Ner s.r.o., CZ
	Phosphatase Inhibitor PhosSTOP Protease Inhibitor cOmplete	Roche Diagnostic Corporation, Switzerland
Protein quanti-fication	Bovine Serum Albumin (BSA) Bradford Reagent (B6916)	Sigma-Aldrich, USA
	Peggy Sue or Sally Sue Mouse Size Master Kit (12-230 kDa)	ProteinSimple, USA
	Primary Antibody for CYP3A4 (sc-53850; 200 µl/ml; mouse monoclonal) Primary Antibody for β-Aktin (sc-47778; 200 µl/ml; mouse monoclonal) Primary Antibody for MDR1 (P - glycoprotein) (sc-55510; 200 µl/ml; mouse monoclonal)	Santa Cruz Biotechnology, USA

Solutions:

Luciferase Substrate:

5 mg D-luciferin

9,6 mg ATP

6,38 mg Coenzyme A

168 mg DTT

1,32 ml TRIS-acetate (1mol/l; pH = 7,8)

1,23 mg EDTA

30,3 mg MgSO4•7H2O

fill into the volume of 30 ml with

ddH2O

Lysis buffer for protein isolation (pH = 7,5):

50 mM HEPES

5 mM EDTA

150 mM NaCl

1%Triton X-100

3.1.2 Equipment

Tab. 2: List of used devices.

Machine	Manufacturer
Centrifuge 5415R	Eppendorf, CZ
Culture incubator Mitre 4000 series	Contherm, New Zeland
Deep Freezer VXE 380	Jouan, France
Dry bath incubator	Major science, USA
Flake Ice making machine F100	Compact, CZ
Laminar box Labculture® Class II Type A2	ESCO, USA
Ligt Cycler 480 II	Roche, Switzerland
Minifuge	Labnet International, USA
Microscope NIB-100	Olympus
NanoDrop LITE Spectrophotomether	Thermo Scientific, USA
Simple Western Sally Sue	ProteinSimple, San Jose, CA, USA
Spectrophotometer Infinite M200	Tecan, Schoeller, CZ
Scales	KERN ABS, USA
Refrigerator A+	Gorenje, Slovenia
Vortex	Heidolph, Germany
Water bath	LabTech Co., CZ

3.1.3 Cell material, plasmids, and primers

Human Caucasian cell line LS180 derived from Duke's type B colorectal adenocarcinoma (ECACC; 87021202).

Expression plasmid for human PXR (pSG5-hPXR) was provided by Dr. S. Kliewer, (University in Texas, Dallas) and chimera p3aA4-luc reporter construct (containing the basal promoter -362/+53 with proximal PXR response element and distal xenobiotic responsive enhancer module -7836/7208 of CYP3A4 gene 50 flanking region inserted to pGL4.10-Basic reporter vector) was described previously in (Pavek *et al.*, 2010).

Tab. 3: List of used oligonucleotides.

Primer	Sequence
CYP3A4 Forward	TGTGTTGGTGAGAAATCTGAGG
CYP3A4 Reverse	CTGTAGGCCCCAAAGACG
GAPDH Forward	CTCTGCTCCTCCTGTTCGAC
GAPDH Reverse	ACGACCAAATCCGTTGACTC
MDR1 Forward	CCTGGAGCGGTTCTACGA
MDR1 Reverse	TGAACATTCAGTCGCTTTATTTCT

3.2 Methods

3.2.1 Cultivation, Trypsinization, and Cell counting

Adherent intestinal epithelial cells were cultured in Dulbecco's modified Eagle's medium (4,5 g/l glucose), enriched with 4 mM L-Glutamine, 1 % non-essential amino-acids and 10 % fetal bovine serum, in sterile plastic cultivation bottles. These bottles were kept in incubator, where the temperature was set at 37°C, atmosphere was fully humidified and contained at 5 % CO_2. Every third day, old medium was discarded, cells were rinsed with 5 ml of phosphate buffered saline, then the cells were treated with 0,25 % trypsin solution for 4 minutes while kept in incubator. When intercellular connections were broken down and cells were separated from the surface of the cultivation bottle, 9 ml of fresh medium was added to the reaction and cells were fully resuspended. A volume of 10 µl of the cell suspension was mixed with 90 µl of trypan blue solution (0,4 % w/v) and applied on Bürker's chamber (2x). The number of cells was counted in at least 10 squares and arithmetic mean was calculated.

The capacity of Bürker's chamber is 0,1 mm^3 e.g. 0,1 µl. To obtain the numeral which represented the number of cells in 1 ml of the cell solution, the determined arithmetic mean was multiplied by dilution factor 10^5 (10^4 corresponding to the unit transfer and 10 corresponding to the previous dilution). Approximately, 4 million of cells were planted into 20 ml of new fresh DMEM and maintained in incubator with stable conditions described above.

3.2.2 Cytotoxicity testing

Cells were trypsinized, counted and planted on sterile 96-well plate, each well containing 50 x 10^3 cells in 200 µl of culture medium. After an overnight adaption of the newly planted cells in incubator, medium was removed and human colorectal adenocarcinoma cell line LS180 was treated with increasing concentrations of graphene oxide (GO) from 0,002 to 20 µg/ml with three groups of different sizes of nano-particles (50-200 nm, 200-500 nm, >500 nm) resuspended in DMEM. A non-ionogenic detergent Triton - X100 (0,1 %) and DMEM were used as positive and negative controls. respectively. On the third day, medium was discarded and 100 µl of MTT in DMEM (0,3 mg/ml) was added to the cells in each well and incubated for 20 minutes. Afterwards, MTT solution was carefully discarded and replaced by dimethyl sulfoxide (DMSO) for dissolution of the formazan crystals. After 15 minutes, an absorbance was measured at 540 nm with Infinite M200 (TECAN, CZ).

3.2.3 Reporter Gene Assay

Transiently transfected human colorectal adenocarcinoma cells (LS180) were used for the assessment of PXR transcriptional activity. For reporter gene assays the DMEM was supplemented with charcoal-stripped fetal bovine serum (CS-FBS DMEM). Cells were trypsinized, counted and planted on 96-well plate. Each well containing 5 x 10^4 cells, 30 ng of pSG5-hPXR, 75 ng of chimera p3aA4-luc reporter construct, 5 µl DMEM without additives and 0,3 µl of Fugene HD, in 200µl of DMEM. Firstly, expression plasmids pSG5-hPXR and reporter vectors p3A4-luc were mixed in 5 µl of DMEM, and then Fugene HD, the lipofection agent, was added subsequently amd incubated for15 minutes at room temperature. The prepared mixture was then added to cell suspension, carefully stirred, and sowed on 96-well plate. Cells were stabilized for 16 hours in incubator and then treated with GO, rifampicin (RIF, 10 µM) or DMSO (0,1% v/v) in FBS-CS DMEM. After 24 hour-incubation, medium was discarded, cells were rinsed with cooled PBS, lysed with 30 µl/well of Reporter lysis 5x buffer and frozen in -80 °C for at least 30 minutes. Defrosting took place at room temperature on a table-shaker and then cells were scraped from the surface and well resuspended. To a volume of 3 µl of cell lysate transferred to black 96-well Nunc microplate, a volume of 30 µl of luciferase substrate was added and luciferase activity was measured with Infinite M200 (TECAN, CZ).

3.2.4 RNA extraction and cDNA synthesis

Total RNA was extracted using TRI Reagent according to manufacturer's instructions. Cells were trypsinized, counted and sowed on the 6-well plate, each well containing 10^6 cells in 2 ml of CS-FBS DMEM. Cells were stabilized for 16 hours in incubator and then treated with GO, rifampicin (RIF, 10 µM) or DMSO (0,1 % v/v) in CS-FBS DMEM. After 24 hour-incubation, medium was discarded, cells were rinsed with cooled phosphate buffer and then RNA was isolated with TRI Reagent. RNA concentration was measured on NanoDrop spectrophotometer and the purity of obtained RNA was evaluated by absorbance ratio at 260/280 nm. cDNA was synthetized from 1 µg of total RNA using M-MuLV Reverse Transcriptase. The reaction was carried out in 12 µl reaction volume. To each sample containing 1 µg of total RNA in 5 µl of RNase free H_2O, 1 µl of random hexamers (100 pmol/µl) was added. Samples were incubated at 65°C for 5 minutes, chilled on ice and centrifugated shortly.

Then to each well, reaction mixture containing 0,6 µl of M-MuLV reverse transcriptase, 0,3 µl of RNase inhibitor, 0,6 µl of 10 mM dNTP, 1,2 µl of 10 x reaction buffer and 3,3 µl of RNase free water, were added. Samples were shortly centrifugated and incubated in at 42 °C for 60 minutes and at 65 °C for 10 minutes. cDNA samples were chilled on ice, a volume of 48 µl of RNase/DNase free water was added to each sample and then stored at -20 °C.

3.2.5 Quantitative Real-Time Polymerase Chain Reaction

The qRT-PCR was performed using 5 µl of probe master, 0,8 µM forward + reverse primer 10 µM; 0,2 µl UPL Probe; 2 µl nuclease free- water and 2 µl of diluted cDNA. Oligonucleotides sequences are listed in Table. 3. Reactions were set in 10 µl volume in triplicates. PCR cycles were set for initial denaturation at 95 °C for 10 minutes, followed by 45 cycles of amplification (denaturation at 95 °C for 10 s, amplification at 60 °C for 30 s), with a final extension at 40 °C for 30 s. Data normalization was carried out using housekeeping gene *GAPDH* and expression values were calculated using delta-delta method.

3.2.6 Quantification of protein expression

LS180 cells were trypsinized, counted and sowed on the 6-well plate, each well containing 10^6 cells in 2 ml of CS-FBS DMEM. Cells were stabilized for 16 hours in incubator and then treated with GO, rifampicin (RIF, 10 µM) or DMSO (0,1 % v/v) in FBS-CS DMEM. After 48 hour-incubation, medium was discarded, cells were rinsed with cooled phosphate buffer. Additionally, 1 ml of cooled PBS was added to each well and cells were scraped from the surface, well resuspended and harvested into microtubes. Samples were centrifuged for 3 min at 5000 RPM at 4 °C and supernatant was discarded. Cells were lysed with 160 µl/sample of ice-cold protein lysis buffer containing anti-protease and anti-phosphatase inhibitors (1x PhosSTOP; 1x cOmplete; 10 ml of protein lysis buffer). The mixture was slightly vortexed, centrifuged for 13 minutes at 13000 RPM at 4 °C and supernatant was transferred into new microtubes. Protein concentration was determined using the Bradford reagent. The Sally Sue Simple Western System was used for protein separation and immunoblot analysis according to the manufacturer's instructions (ProteinSimple™). Reagents were obtained from ProteinSimple (San Jose, CA, USA) and prepared according to the manufacturer's

recommendations (http://www.proteinsimple.com/sally_sue.html). Firstly, samples were diluted to adjust the protein concentration to 1 µg/µl in 5 µl with sample buffer.

Aliquot of 1.25 µl of the 5× master mix (ProteinSimple) was added into final concentration of 1× sample buffer, 1× fluorescent molecular weight markers, and 40 mM DTT. Samples were then heated at 37 °C for 20 min. The samples, wash buffer, blocking reagent, primary/secondary antibodies and chemiluminescent substrate were dispensed into wells in the manufacturer-provided microplate. To detect proteins of our interest, primary monoclonal antibodies against CYP3A4 protein, P-glykoprotein and β-Actin were used. For CYP3A4 detection the primary antibody was diluted 1:10, for P-gp 1:1000 and for β-Actin detection 1:1000. The secondary antibody was part of ProteinSimple Kit and was not diluted. Thereafter, the electrophoretic separation of proteins of and immune-detection steps took place in the system of capillaries and were fully automated. Western analysis was performed at room temperature, and instrument default settings were used. The data were analyzed using provided Compass software (ProteinSimple). Normalization of the peak area of P-gp and CYP3A4 protein was carried out with reference to the peak area of β-Actin protein in the same sample.

4. Results

4.1 Cytotoxicity of graphene oxide

The potential cytotoxic effect of graphene oxide on LS180 cell line was studied. The MTT test was used to determine the cytotoxicity of GO. This test is based on a fact, that only alive (metabolically active) cells, due to mitochondrial dehydrogenases, are able to reduce yellow tetrazolium salt/dye to purple formazan. The number of survival cells, so called viability, was measured spectrophotometrically at wavelength 570 nm and normalized to negative control (DMSO, 0.1 % v/v). A nonionic detergent, the Triton X-100 (0,1 %) was used as a positive control. Cells treated with Triton X-100 died, therefor were not able to reduce the MTT salt, the cell suspension remained yellow, the viability was 0 %.

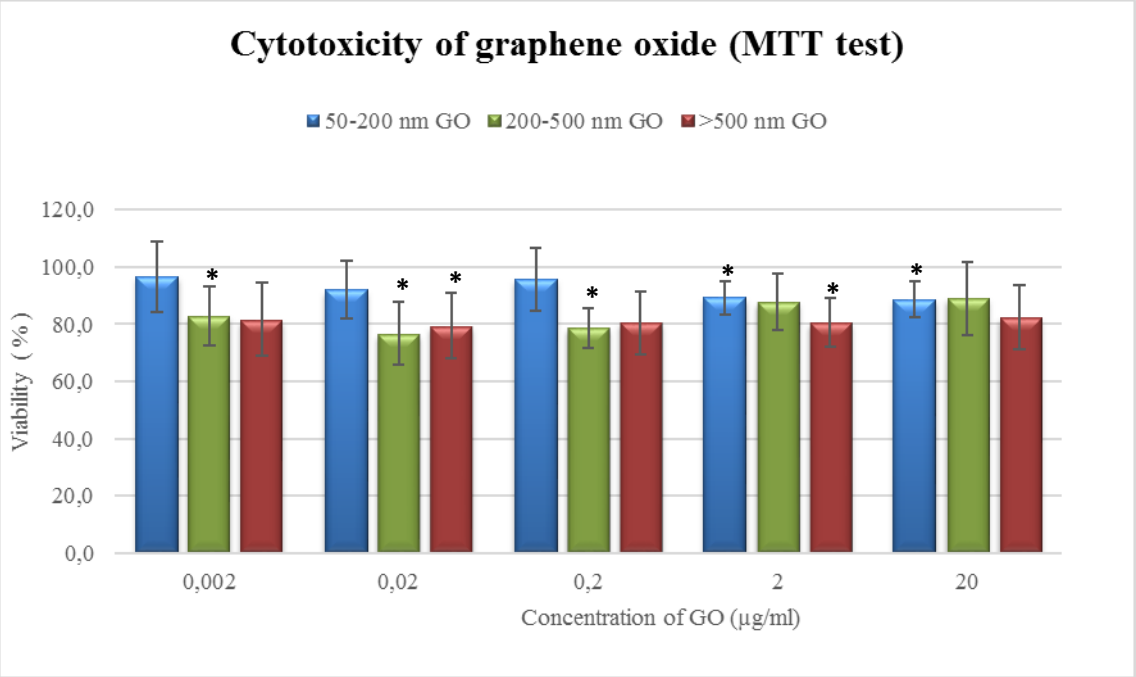

Fig. 10: Cytotoxicity of graphene oxide.
LS180 cells were treated for 24 hours with different concentrations of GO; range 0,002 µg/ml to 20 µg/ml. Untreated LS180 cells were used as negative control and represent 100 % of viability (not shown). Triton X-100 was used as positive control and represents 0 % viability (not shown). The number of living cells (viability) was detected with MTT test. Data were expressed as a mean of at least four biological replicates ± SD. Each experiment was performed in tetra-plicate. Statistical significance was evaluated by Student t-test. * - P <0,01.

Considering the effect of nanoparticles with size from 50 to 200 nm, no intense decline in viability was observed (max. 10 %) among the different concentrations of GO (Fig. 10). On the other hand, bigger nanoparticles of GO (such as 200-500 nm or >500 nm) influenced the number of living cells a bit more than GO 50-200 nm (Fig. 10). An approximately 20 % decrease in viability was observed in LS180 cells after a treatment with nanoparticles of GO with size range 200-500 nm (concentration range from 0,002 μg/ml to 0,2 μg/ml) (Fig. 10). Higher concentrations of GO (200-500 nm) such as 2 μg/ml and 20 μg/ml caused a 10 % declination in viability (Fig. 10). The biggest of investigated graphene oxide nanoparticles (size >500 nm) seemed to have quite the same effect on LS180 cell line viability among all examined concentrations. The constant decrease in viability was approximately 20 %. The results are statistically significant (Fig. 10).

Graphene induced adsorption, optical interferences, as well as electron transfer can prevent to appropriate evaluate graphene toxicity. The importance of careful interpreting of obtained data from classical *in vitro* assays on assessment of graphene cytotoxicity was demonstrated (Jiao *et al.*, 2015). Therefore, light microscopy images of LS180 cells treated by GO are presented in figures 11 A-C. The morphology of LS180 cell line was not affected by GO treatment. Based on the above-mentioned facts, concentrations up to 20 μg/ml were used ensuring ≥ 80 % cell survival.

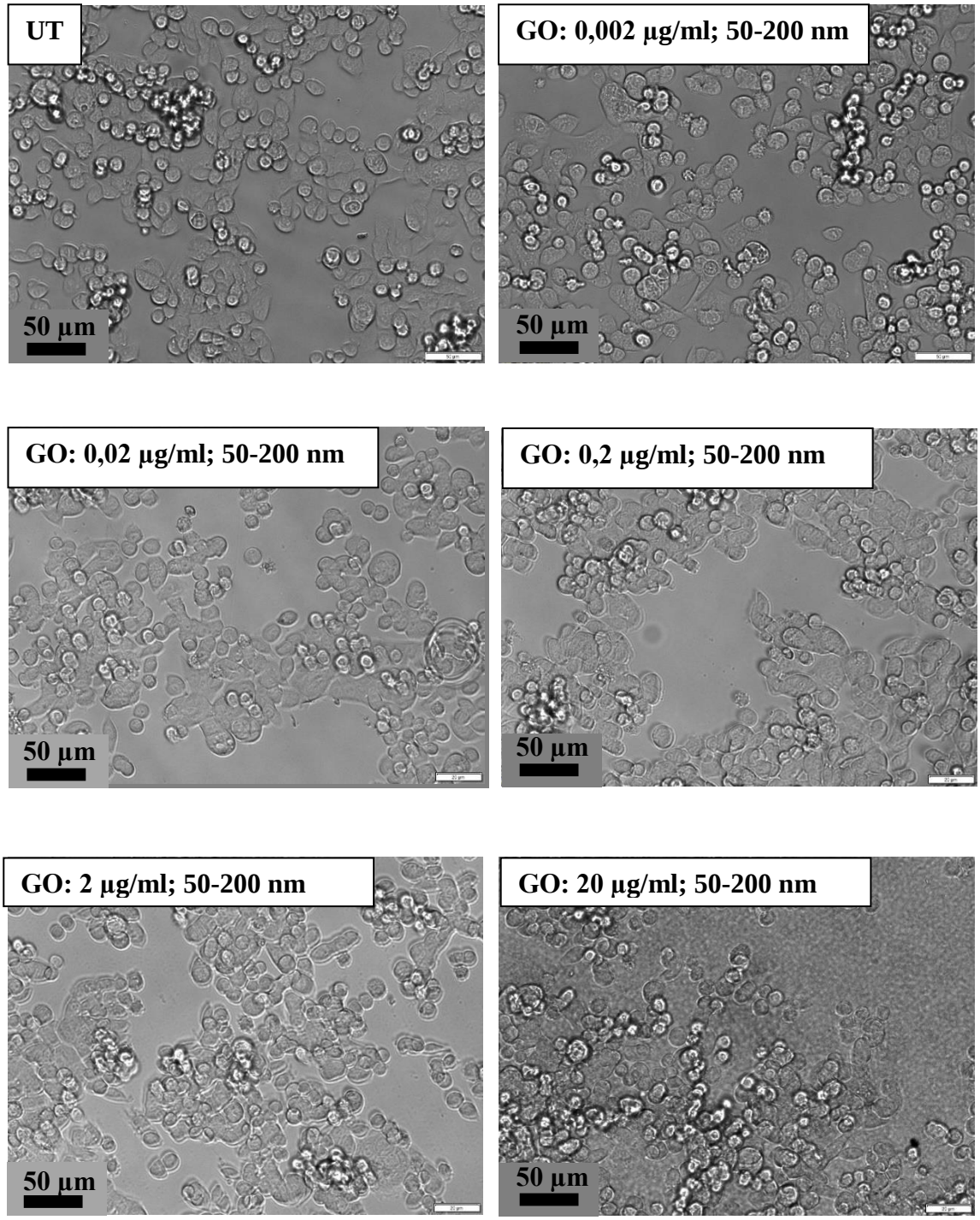

Fig. 11A: Morphology of LS180 cells after graphene oxide treatment.
Light microscopy images of LS180 cells, which were treated for 24 hours with different concentrations (range 0,002 µg/ml to 20 µg/ml) of GO nanoparticles with size 50-200 nm, were presented. Magnification 200x.

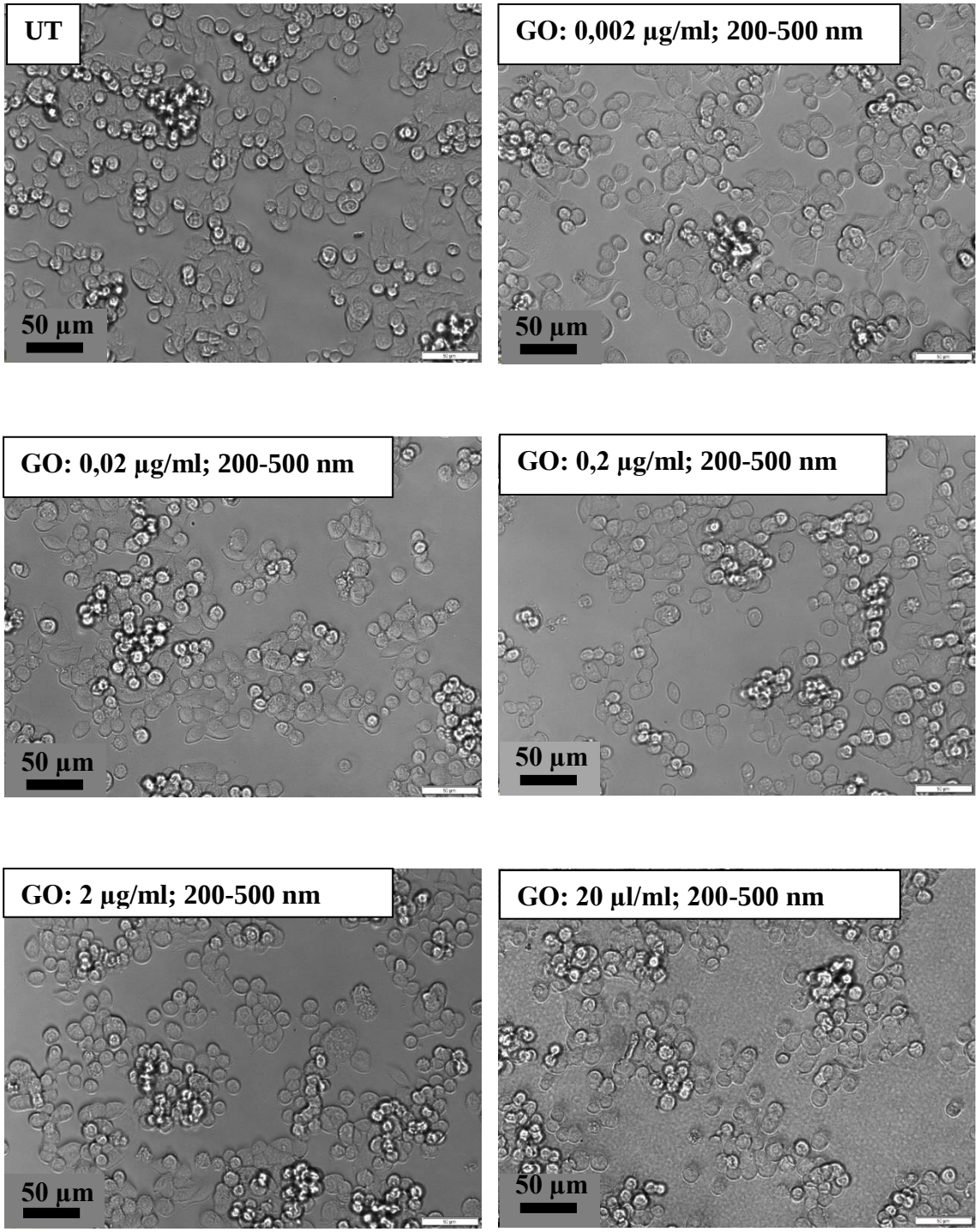

Fig. 11B: Morphology of LS180 cells after graphene oxide treatment.
Light microscopy images of LS180 cells, which were treated for 24 hours with different concentrations (range 0,002 µg/ml to 20 µg/ml) of GO nanoparticles with size 200-500 nm, were presented. Magnification 200x.

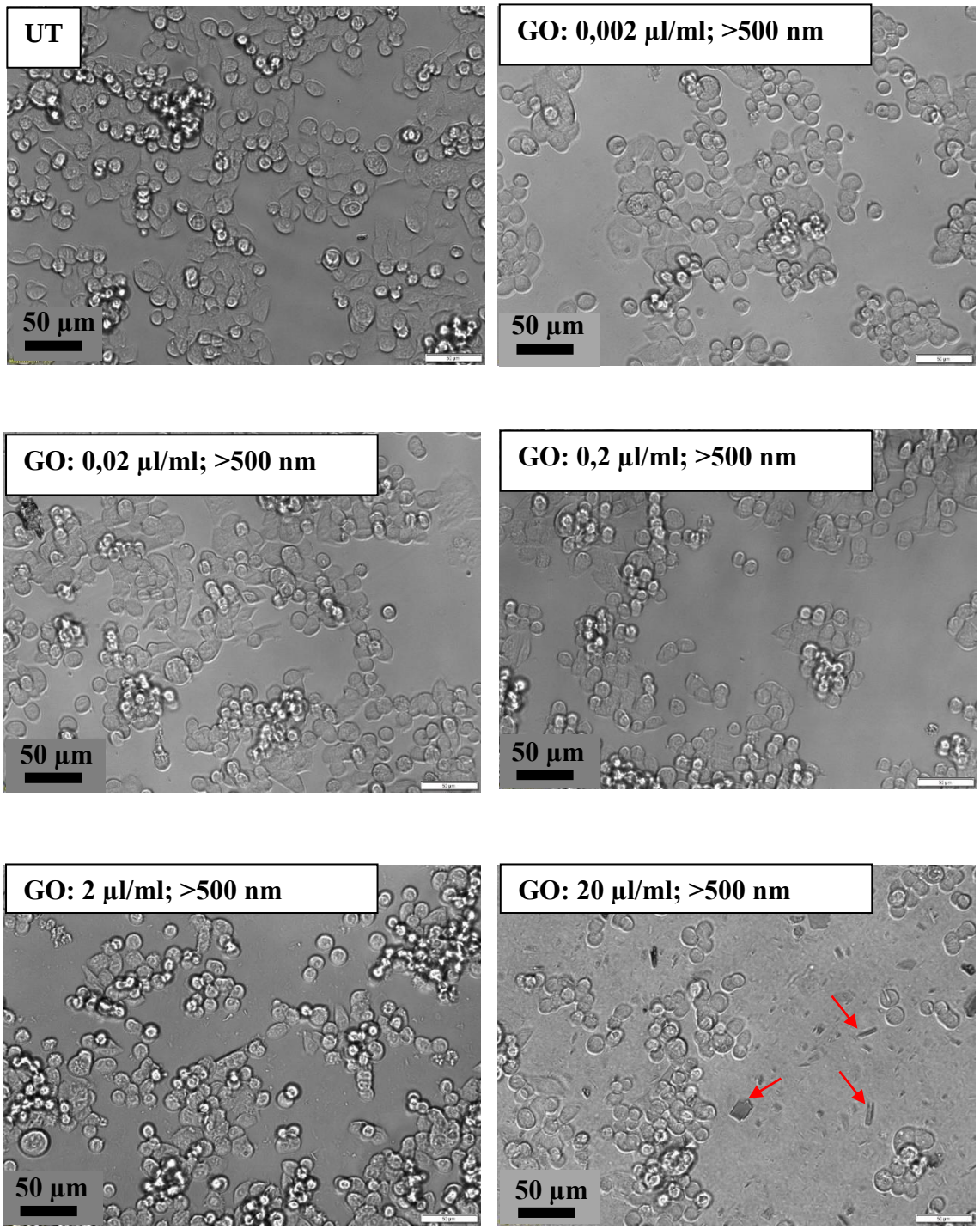

Fig. 11C: Morphology of LS180 cells after graphene oxide treatment.
Light microscopy images of LS180 cells, which were treated for 24 hours with different concentrations (range 0,002 µg/ml to 20 µg/ml) of GO nanoparticles with size >500 nm, were presented. Magnification 200x. Arrows point at the GO nanoparticles.

4.2 Transactivation of *CYP3A4* promoter by PXR

The effect of graphene oxide on nuclear pregnane receptor (PXR) signalization was examined in LS180 cell line by reporter gene assay. The cells were transiently co-transfected with plasmid carrying PXR-gene (pSG5-hPXR) and reporter vector (p3A4-luc), where the CYP3A4 promotor was inserted and followed by the gene coding for luciferase. In these transiently transfected cells, PXR is overexpressed, therefor PXR-signaling pathway is intensified. In the case of PXR activation, PXR binds to CYP3A4 promoter and induce the gene expression. The amount of reporter gene product, in our case the luciferase, is directly proportional to transcriptional activity of PXR. For luciferase detection, intensity of luminescence was recorded.

Activation of PXR is expressed as fold induction - the ratio of luminescence measured in sample to luminescence observed in untreated cells UT (in agonistic mode) or as % of maximal induction - the ratio of luminescence measured in sample to luminescence observed in cells treated with PXR ligand rifampicin, multiplied by one hundred (in antagonistic mode).

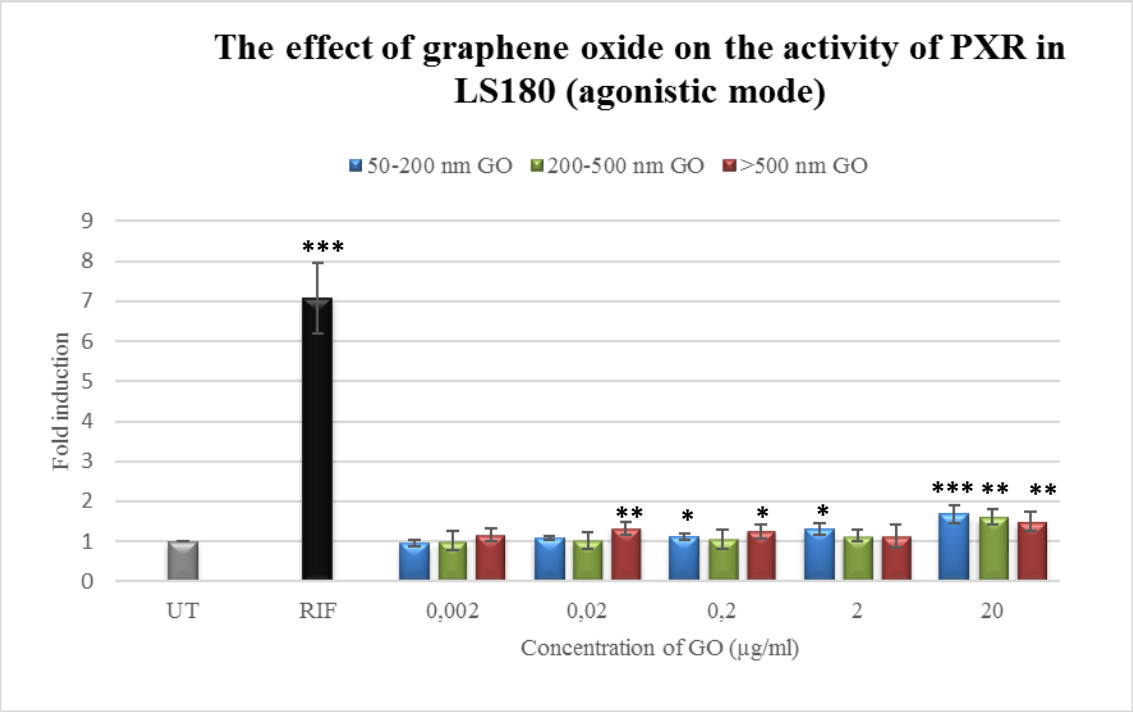

Fig. 12: Concentration-dependent effect of GO on PXR activity (agonistic mode).
LS180 cells were treated for 24 hours with different concentrations of GO; range 0,002 µg/ml to 20 µg/ml. Untreated LS180 cells (UT) were used as negative control. A ligand of PXR, rifampicin (RIF, 10µM), was used as positive control. Data were expressed as a mean of at least three biological experiments, each performed in four technical replicates ± standard deviation (SD) and normalized to negative control UT (set to 1). Statistical significance was evaluated by Student t-test. * - P <0,05; ** - P <0,01; *** - P <0,001.

Rifampicin significantly (average of 7-fold) induced the CYP3A4 promotor trans-activation (Fig. 12). Activation of PXR by RIF confirmed that our reporter gene system is functional. In comparison to RIF, graphene oxide itself slightly but in some cases significantly influenced the luciferase level in transiently transfected LS180 cells. Data showed that among all examined sizes of GO nanoparticles, the concentrations 0,002 µg/ml; 0,02 µg/ml; 0,2 µg/ml and 2 µg/ml did not influence the reporter gene expression while the highest used concentration, 20 µg/ml, caused very slight, but statistically significant increase (1,7 ± 0,2 for GO 50-200 nm, 1,6 ± 0,2 for GO 200-500 nm and 1,5 ± 0,2 for GO>500 nm) (Fig. 12).

To examine the possible antagonistic involvement of graphene oxide in PXR-mediated signaling, the cells were treated with GO and rifampicin (PXR agonist) at the same time. All examined concentrations of GO nanoparticles with size 50-200 nm showed not to influence the CYP3A4 promoter trans-activation by RIF (Fig. 13).

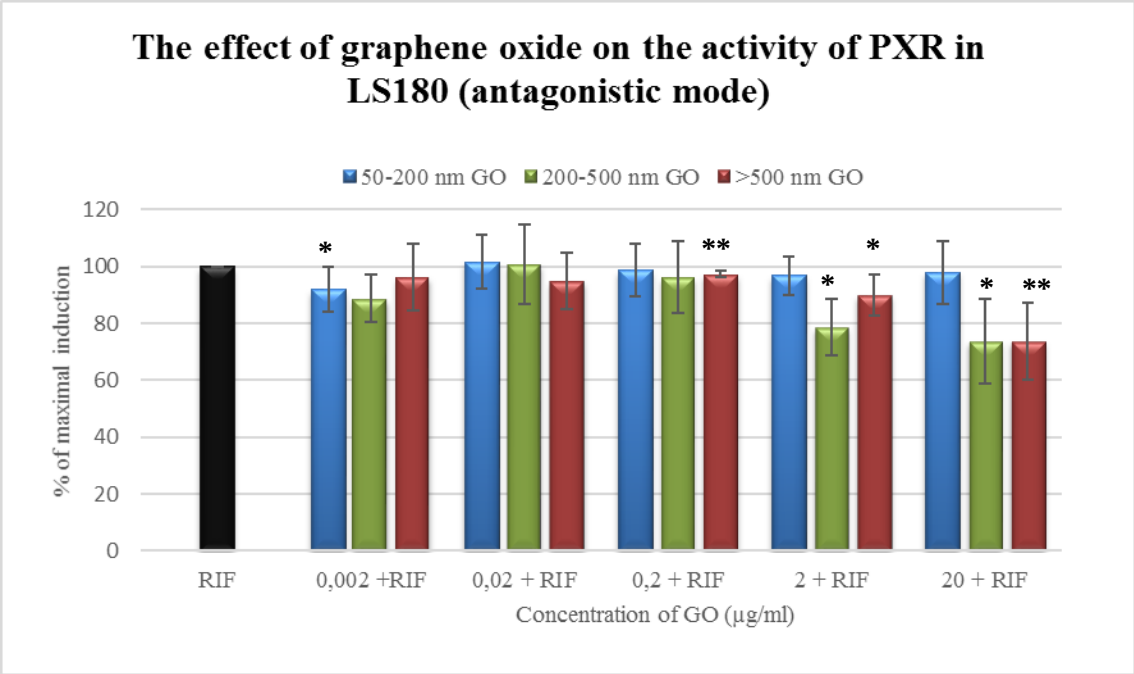

Fig. 13: Concentration-dependent effect of GO on PXR activity (antagonistic mode).
LS180 cells were treated for 24 hours with different concentrations of GO; range 0,002 µg/ml to 20 µg/ml in combination with 10 µM rifampicin. Untreated LS180 cells (UT) were used as negative control (not shown). A ligand of PXR, rifampicin (RIF, 10µM), was used as positive control and represented 100 % induction of reporter gene expression, in our case coding for luciferase. Data are expressed as a percentage of maximal activation attained by RIF ± standard deviation (SD). Data were expressed as a mean of at least three biological replicates, each performed in four technical replicates. Statistical significance was evaluated by Student t-test.
* - P <0,05; ** - P <0,01.

Differentially, GO nanoparticles with size 200-500 nm caused a significant decrease (22 % and 26 %) in PXR-mediated luciferase activation for concentration 2 and 20 μg/ml (Fig. 13). The trend of GO effect on RIF-inducible PXR-mediated luciferase activity was quite alike in nanoparticles with size 200-500 and >500 nm (Fig 13). Specifically, concentrations 2 μg/ml and 20 μg/ml (>500 nm) caused a declination 10 % and 26 % (Fig. 13). Here, we observed the antagonistic effect of GO nanoparticles (200-500 nm; >500 nm) on the rifampicin activated PXR signaling. Due to known limitations of MTT test for evaluation of graphene cytotoxicity and the absence of a normalization step in the gene reporter assay, our findings require further investigations.

4.3 Effects of GO nanoparticles on the expression of PXR target genes at the mRNA level

Further, the effect of graphene oxide on the PXR signaling pathway was examined in LS180 cell line by studying the expression of PXR-regulated genes, namely *CYP3A4* and *MDR1*. To investigate the mRNA levels, the quantitative Real-Time Polymerase Chain Reaction was used. This method is quick, super-sensitive and highly specific. Based on fluorescent dyes or probes bound to template, it allows us to detect small differences in the number of amplicons and monitor the reaction progress in real-time.

In most cases, GO itself did not affect the gene expression of *CYP3A4* (Fig. 14). No matter what concentration or size of GO particles was used, the amount of CYP3A4 transcript remained pretty much the same as it was observed in untreated cells (Fig. 14). In contrast to GO, the positive control rifampicin, caused a significant increase (approximately 3-fold) in *CYP3A4* gene expression (Fig. 14).

Combined treatment of LS180 cells with GO and PXR agonist rifampicin revealed a slight antagonistic involvement of graphene oxide in PXR-mediated signaling (Fig. 14). Except the smallest and medium-size GO NPs (50-200 nm; 200-500 nm) at the lowest concentration (0,2 μg/ml), all examined GO nanoparticles decreased the induction of *CYP3A4* gene expression by RIF (Fig. 14). The decline in RIF-induced *CYP3A4* gene expression was around 5 %, 24 % and 16 % in cells treated with the increasing dose of the smallest GO particles (50-200 nm). Medium-size particles (200-500 nm) decreased the expression around 25 % except the lowest concentration and the biggest particles decreased the expression dose-dependently around 19 %, 15 % and 33 % (Fig. 14)

In addition to the *CYP3A4*, we also studied the multidrug resistant protein *(MDR1)* also known as P-glycoprotein (P-gp). Since this transporter is responsible for decreasing the intracellular concentration of many drugs, therefore naturally limiting their therapeutic effect, the monitoring of *MDR* is of great importance, especially in development of new drugs or regarding the drug-drug interactions. After exposing the LS180 cells to graphene oxide nanoparticles, no significant change was detected in the *MDR1* mRNA level (Fig. 15). While, in the case of rifampicin treatment, the PXR agonist, a significant increase (approximately 4-fold) in *MDR1* gene expression was observed (Fig. 15).

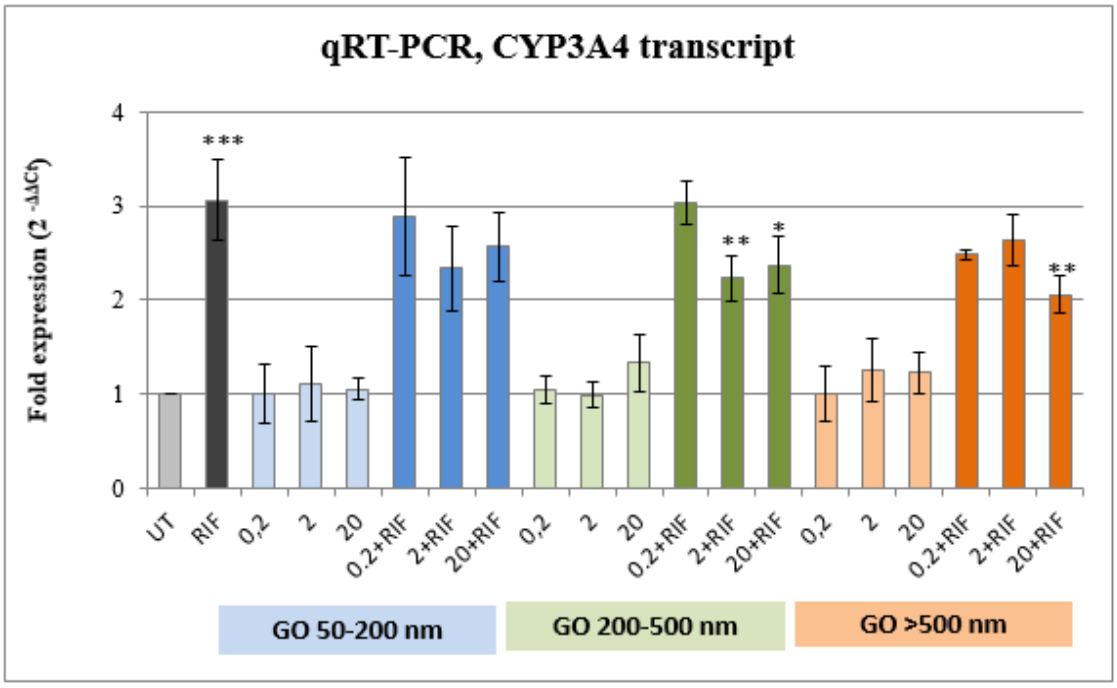

Fig. 14: The effect of GO on the expression of *CYP3A4* gene studied by Quantitative Real-Time Polymerase Chain Reaction.
The graph represents the relative gene expression of *CYP3A4* gene in LS180 cells treated for 24 hours with different concentrations of GO; range 0,2 µg/ml to 20 µg/ml. Untreated LS180 cells (UT) were used as negative control and a ligand of PXR, rifampicin (RIF, 10 µM), was used as positive control. Expression data were normalized to the housekeeping gene *GAPDH* and processed by delta-delta method. Data were expressed as mean of at least three independent biological experiments ± standard deviation (SD), each PCR run was performed in three technical replicates. Data were normalized to negative control UT (set to 1). Statistical significance was evaluated by Student t-test. * - P <0,05; ** - P <0,01; *** - P <0,001. In agonistic mode, the statistical significance was compared to UT and in antagonistic mode, the statistical significance was compared to RIF.

Exposing the LS180 cells to graphene oxide led to dose-dependent and statistically significant decrease in RIF-induced *MDR1* gene expression. The decrease in *MDR1* gene expression was approximately 25 %, 44 % and 36 % in cells treated by the increasing dose of the smallest GO particles (50-200 nm). Medium-size particles (200-500 nm) decreased the expression around 40 % except the lowest concentration and the biggest particles (>500 nm) decreased the expression dose-dependently around 24 %, 34 % and 41 % (Fig. 15).

Comparing the effect of GO on RIF-induced *MDR1* and RIF-induced *CYP3A4* gene expression, the decrease in the *MDR1* gene expression was more intense, nevertheless, the trend was the same in both PXR-driven genes.

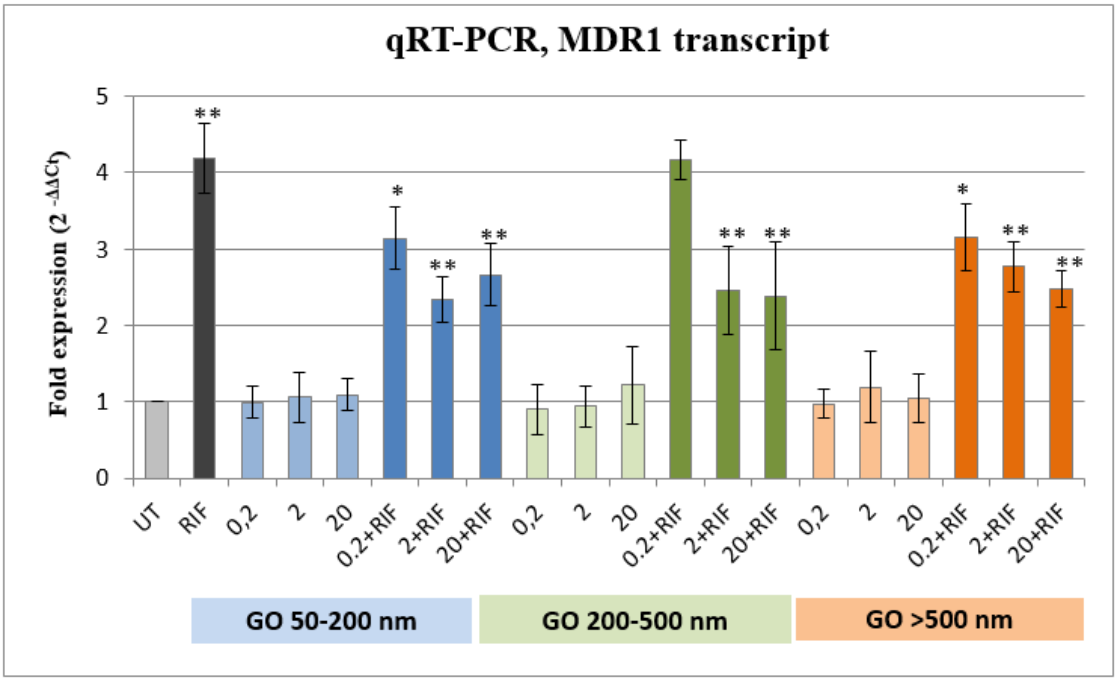

Fig. 15: The effect of GO on the expression of *MDR1* gene studied by Quantitative Real-Time Polymerase Chain Reaction.
The graph represents the relative gene expression of *MDR1* gene in LS180 cells treated for 24 hours with different concentrations of GO; range 0,2 µg/ml to 20 µg/ml. Untreated LS180 cells (UT) were used as negative control and a ligand of PXR, rifampicin (RIF, 10 µM), was used as positive control. Expression data were normalized to the housekeeping gene *GAPDH* and processed by delta-delta method. Data were expressed as mean of at least three independent biological experiments ± standard deviation (SD), each PCR run was performed in three technical replicates. Data were normalized to negative control UT (set to 1). Statistical significance was evaluated by Student t-test. * - P <0,05; ** - P <0,01; *** - P <0,001. In agonistic mode, the statistical significance was compared to UT and in antagonistic mode, the statistical significance was compared to RIF.

4.4 Effects of GO nanoparticles on the expression of PXR target genes at the protein level

Thereafter, the possible influence of graphene oxide on the PXR signaling pathway was studied at the protein level of PXR-driven genes like *CYP3A4* and *MDR1*. The capillary SDS-PAGE separation followed immobilization of proteins on the capillary wall, then by immunodetection with specific antibodies using Sally Sue was performed in order to investigate the protein abundance,

Graphene oxide itself increased the level of CYP3A4 protein in LS180 cell line in most cases (Fig. 16). The increment was comparable with the induction observed in LS180 cells treated with PXR agonist rifampicin (Fig. 16). The strongest GO impact was detected among medium-size GO nanoparticles (Fig. 16). The smallest GO nanoparticles (50-200 nm) up-regulated the CYP3A4 protein level 2x (0,2 μg/ml; 2 μg/ml), although the highest concentration (20 μg/ml) caused slight decrease in CYP3A4 protein level (Fig. 16). The effect of medium-size GO nanoparticles (200-500 nm) was interestingly high. Here we observed the increment to 3-fold (0,2 μg/ml); 2,7-fold (2 μg/ml) and 3,9-fold (20 μg/ml) (Fig. 16). The third category of studied GO nanoparticles (>500nm) caused approximately 2-fold (0,2 μg/ml and 2 μg/ml) and 1,6-fold induction (20 μg/ml) in CYP3A4 protein level (Fig. 16).

When LS180 cells were co-treated with GO and a PXR ligand rifampicin, the level of CYP3A4 protein remained pretty much the same as detected in cells treated with RIF itself (except the medium-size nanoparticles). The smallest GO particles (50-200 nm) did not influence the inducible CYP3A4 protein level, only the concentration 0,2 μg/ml stimulated the CYP3A4 protein level to 3-fold. Nevertheless, this phenomenon was not observed in other experiments so this rise was not significant (Fig. 16). A distinct behavior was monitored among medium-size GO nanoparticles. Here, in contrary with GO 50-200 nm and >500 nm, a decline in RIF-promoted induction of CYP3A4 protein expression was observed (Fig. 16). Medium-size particles (200-500 nm) at concentration 0,2 μg/ml caused almost 75 % drop of CYP3A4 protein level compared to RIF (Fig. 16). Higher concentrations (2 μg/ml and 20 μg/ml) of medium-size GO nanoparticles caused only slight decrease of CYP3A4 protein level compared to RIF. After the treatment with the biggest studied GO nanoparticles (>500 nm) and rifampicin at the same time, the levels of CYP3A4 protein were approximately same as observed in cells treated with rifampicin itself (Fig. 16).

An increment of CYP3A4 protein level after 2 µg/ml GO (>500 nm) + RIF co-treatment was not statistically significant.

When studying the effect of graphene oxide on P-glycoprotein (the product of *MDR1* gene) in LS180 cell line, we observed that GO itself increased the level of P-gp in size-dependent manner (Fig. 17). The increment of P-gp level was more intense with bigger size of GO nanoparticles (Fig. 17). Also with higher concentration of GO nanoparticles, the induction of P-gp expression moderately declined (Fig. 17). The induction of P-gp level in concentration 0,2 µg/ml increased after the treatment with the smallest of examined GO nanoparticles (50-200 nm) to 1,6-fold, after medium-size GO nanoparticles (200-500 nm) to 2,4-fold (0,2 µg/ml), and the biggest of tested GO nanoparticles (>500 nm) caused an increment to 4,2-fold. The application of higher concentration (2 µg/ml) let to an increment to 1,3-fold (50-200 nm), 2,1-fold (200-500 nm), and 4,2-fold (>500 nm). The highest tested concentration (20 µg/ml) increased the P-gp level to 1,4-fold (50-200 nm), to 1,8-fold (200-500 nm), and to 3-fold (>500 nm).

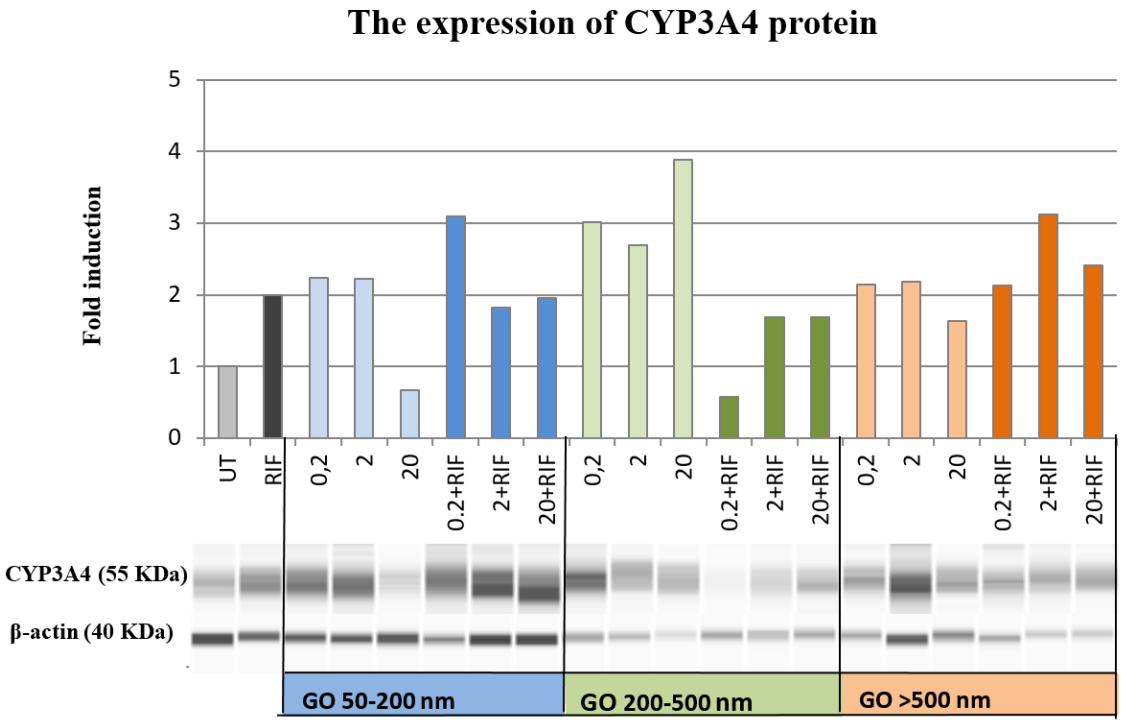

Fig. 16: Representative virtual western blot together with quantification data of CYP3A4 levels obtained from Sally Sue Protein Simple analysis.
LS180 cells were treated for 48 hours with different concentrations of GO; range 0,2 µg/ml to 20 µg/ml in the presence or absence of rifampicin. Untreated LS180 cells (UT) were used as negative control and a ligand of PXR, rifampicin (RIF, 10 µM), was used as positive control. In the bar graph, the data were expressed as a fold induction over untreated cells and normalized to β-actin levels. Here were shown representative results of one from more than three independent biological experiments.

Rifampicin, the PXR agonist, caused a significant increase (5,6-fold) in P-glycoprotein expression (Fig. 17), while only a slight increment (2-fold) was detected in CYP3A4 protein level (Fig. 16) compared to untreated LS180 cells. In antagonistic mode (GO+RIF co-treatment), we observed that graphene oxide stimulated the expression of P-gp induced by RIF and that this induction declined with increasing concentration of GO nanoparticles (Fig. 17). After GO+RIF co-treatment with the smallest GO NPs (50-200 nm), an increase in the RIF-dependent induction of P-gp level to 8,5-fold (0,2 µg/ml), slight decrease to 4,8-fold (2 µg/ml) and to 3,9-fold (20 µg/ml) was detected. Considering the medium-size GO nanoparticles (200-500 nm), slight decrease to 5,15-fold (0,2 µg/ml), slight increment to 7,0-fold (2 µg/ml) and decrease to 4,5-fold (20 µg/ml) was observed in RIF-promoted induction of P-gp level. When the LS180 cells were co-treated with the biggest of tested GO nanoparticles (>500 nm) and RIF at the same time, a strong increment to 9,7-fold (0,2 µg/ml), 8,75-fold (2 µg/ml) was detected in RIF-dependent induction of P-gp level, while there was no obvious change in concentration 20 µg/ml (Fig. 17).

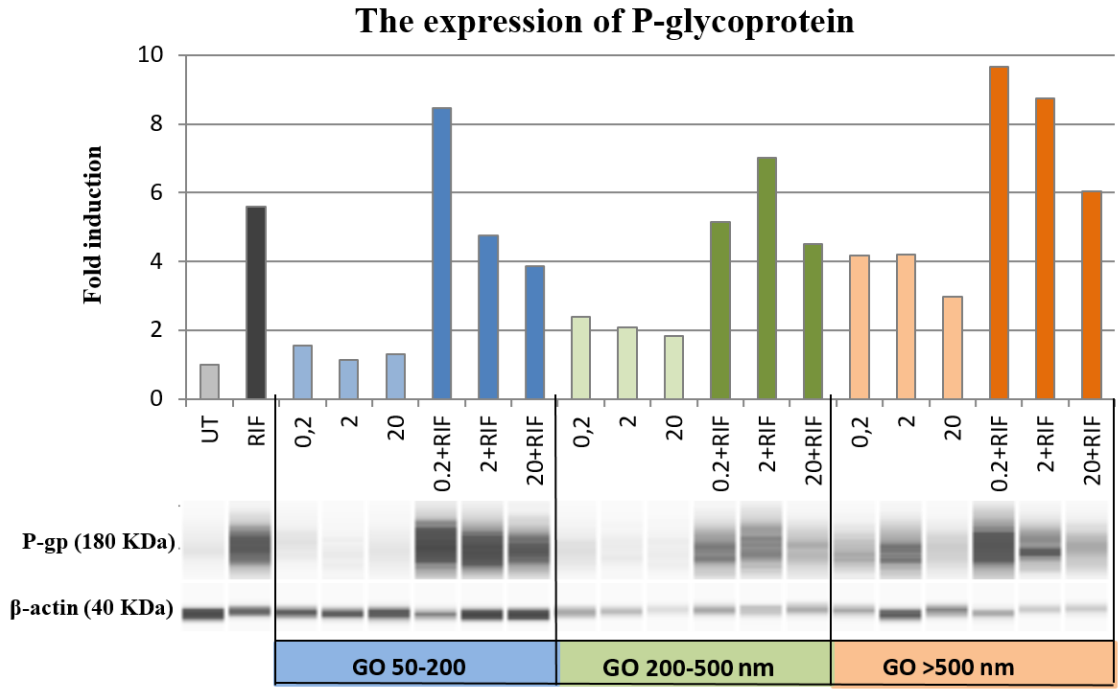

Fig. 17: Representative virtual western blot together with quantification data of P-glycoprotein levels obtained from Sally Sue Protein Simple analysis.
LS180 cells were treated for 48 hours with different concentrations of GO; range 0,2 µg/ml to 20 µg/ml in the presence or absence of rifampicin. Untreated LS180 cells (UT) were used as negative control and a ligand of PXR, rifampicin (RIF, 10 µM), was used as positive control. Band intensities were normalized to β-actin (loading control). The results were normalized to UT. Here were shown representative results of one from more than three independent biological experiments.

Experiments revealed that the GO itself did not influence the *CYP3A4* mRNA level, while the CYP3A4 protein level was increased in most cases. When LS180 cells were co-treated with graphene oxide and rifampicin, the GO caused dose-dependent decrease of RIF-induced *CYP3A4* gene expression. On the other hand, in antagonistic mode, the CYP3A4 protein level slightly increased or remained the same as observed in cells treated with RIF itself.

An important efflux transporter of xenobiotics (MDR1 also called as P-gp) controlled by PXR was also studied. Experiments showed that graphene oxide itself did not influence the *MDR1* mRNA level, whereas the MDR1 protein level was elevated and that the size and concentration of GO played role in this action. The antagonistic mode revealed that GO decreased the RIF-promoted induction of *MDR1* gene expression in dose-dependent manner. With increasing concentration of GO nanoparticles the RIF-induced level of MDR1 protein also decreased.

Graphene oxide influenced PXR-driven genes not only on transcriptional level (antagonistic mode) but also on translational level (agonistic and antagonistic mode) and the effect was size and/or dose-dependent. However, the influence of GO on investigated genes differed at the transcriptional and the translational level in some cases.

5. Discussion

Graphene oxide owns large surface area and contains reactive oxygen functional groups in its structure. This provides high capacity for binding drugs as well as nonpolar pollutants. Since there is a great potential for GO applications, its production strongly increases. This may lead to accidental release of GO-based materials and introduction of a new anthropogenic pollutant into the environment. It was demonstrated, that oxidized graphene nanomaterials can be up-taken by diverse phagocytic and non-phagocytic cells of different origin (Huang *et al.*, 2012, Lammel *et al.*, 2013, Na *et al.*, 2013, Sasidharan *et al.*, 2012, Vila *et al.*, 2012) and serve as effective carrier systems for the targeted delivery of chemical compounds (Liu *et al.*, 2008) and biomolecules like proteins, DNA and siRNA (Bao *et al.*, 2011). Despite the fact, that the research focused on technical and biomedical requests of graphene derivatives is expanding quickly, the information about their interaction with the biological systems or internal toxicity are not sufficient (Sanchez *et al.*, 2012). It was shown that GO in combination with AhR agonists, leads to higher induction of AhR-mediated CYP1A in fish, suggesting that GO can endanger the water organisms by increasing the cellular absorption of organic pollutants due its ability to bind these substances and releasing them intracellularly (Lammel and Navas, 2014).

Since the pregnane X receptor is responsible for cellular response to vast range of exogenous compounds (Kliewer and Willson, 2002, Svecova *et al.*, 2008, Watkins *et al.*, 2001) and also belongs to important regulators of lipid and saccharide homeostasis (Moreau *et al.*, 2008, Rysa *et al.*, 2013), the aim of this study was to find out if the graphene oxide may affect its signaling pathway, which might subsequently lead to disruption the PXR-dependent metabolism of xenobiotics with an impact on human health. Potential hazardous impact of GO was studied with focus on PXR-driven genes, namely *CYP3A4* and *MDR1*.

Firstly, given to many promising bio-medical applications of GO, we studied the possible cytotoxic effect of GO on LS180 cell line by MTT test (Fig. 10). MTT test revealed a decrease (max 25 %) in number of living cells after treatment with graphene oxide, where especially medium-size (200-500 nm) and the biggest (>500 nm) nanoparticles showed to have stronger impact rather than the smallest examined particles (50-200 nm). Among the different examined concentrations of GO (0,002 – 20 μg/ml) no distinctive change was observed. This suggests, that the size of GO

nanoparticles is linked with their effect on LS180 cells viability. Based on the cytotoxicity data and light microscopy images, concentrations up to 20 μg/ml ensuring ≥ 80 % cell survival were used for further examination.

Chang Y. *et al.* (2011) published a systematic study about GO effects on A549 cells, which indicates that GO has good biocompatibility i.e. low toxicity to this lung carcinoma epithelial cell line. It showed that in concentration range 0-100 μg/ml neither the morphology observed by optical microscopy, nor the viability evaluated by CCK-8 assay nor the membrane integrity were significantly changed by GO in A549 cells. However, GO-dependent induction of reactive oxygen species ROS was observed, which may have caused a slight decrease of viability at higher GO concentrations (Chang *et al.*, 2011). Similarly, data obtained in this study showed low effect of GO on LS180 cell line viability (Fig. 10, Fig. 11). In addition to the literature reporting the good biocompatibility of GO (Liu *et al.*, 2008, Zhang *et al.*, 2012), there are reports of GO having a higher toxicity to cells and animals at higher concentrations (Agarwal *et al.*, 2010, Hu *et al.*, 2010b, Wang *et al.*, 2011). For example, Wang *et al.* (2010) found that GO is toxic to human fibroblast cells at the concentration of 50 μg/ml and higher. Likewise, (Liao *et al.*, 2011) reported that graphene oxide showed the hemolytic activity. The inconsistencies in results might originate in the GO synthesis, different GO properties such as size, surface charge, particulate state, surface functional groups, and residual precursors. In general, smaller nanoparticles (150 nm and less) were found to enter the cells more easily, and were also linked with higher levels of ROS and GO-based cytotoxicity. In contrary, we observed that bigger GO particles decreased the viability (Fig. 10).

To correctly evaluate the cytotoxicity of graphene-derived nanomaterials, the choice of cell lines and testing assays is of great importance. It was found that an adsorption, optical interferences, as well as an electron transfer can prevent to appropriate evaluation of graphene toxicity. A major source of spurious results described by previously was the absorption interference of graphene (Creighton *et al.*, 2013). Using cell-free media in MTT test a 10 % decrease and in CKK-8 test almost 30 % reduction of signal detection was observed (Jiao *et al.*, 2015). The graphene adsorption intensity to MTT/CCK-8 was directly proportional to duration of contact, displaying the time-respond. Graphene may adsorb the dye through Π-Π and electrostatic interaction adsorption leading to less formazan salt able to react with cells. Based on these information, we conclude that observed decrease in viability of LS180

cell line could be primarily caused by graphene oxide interference with MTT assay, nonetheless further examinations are necessary.

The effect of graphene oxide particles on pregnane X receptor signaling pathway was investigated on both - gene and protein levels, employing methods such as Reporter Gene Assay, qRT-PCR and western blotting with immunodetection.

Agonistic mode elucidating the effects of graphene oxide itself, showed that GO at lower concentrations (0,002 – 2 μg/ml) had no effect on the induction of PXR-dependent transactivation of CYP3A4 promotor, while the highest tested concentration (20 μg/ml) caused very slight but statistically significant induction (1,5 to 1,7 - fold) (Fig. 12). These data were in good agreement with results from qRT-PCR, where the levels of PXR-driven genes were not changed by GO itself either (Fig. 14, Fig. 15). Lammel *et al.* (2014) also observed that GO alone had no significant influence on *CYP1A* gene expression and enzymatic levels when studying GO effects on topminnow fish hepatoma cell line PLHC-1. In contrary, we observed that the protein level of examined PXR-driven genes was up-regulated in most of the cases (Fig. 16, Fig. 17). Specifically, CYP3A4 protein level increased 2-3x, where medium-size particles had the strongest effect (Fig. 16). The level of P-glycoprotein was upregulated by medium-size and biggest particles (200-500 nm, >500 nm), while no effect was observed among the smallest nanoparticles (50-200 nm) (Fig. 17). Possible explanations why no rise in mRNA level was detected while protein level increased after GO exposure, is that mRNA translation can be upregulated by RNA binding proteins or that translation might be upregulated by downregulation of miRNA targeting the mRNA or that the protein stability might increase due to post-translational modifications. Another possible explanation could be that GO induces ROS formation (Lammel *et al.*, 2013) and may cause disruption of plasma membrane via binding to membrane lipids. This disruption may cause aggregation of P-gp protein level, which likely disrupted degradation. This idea might be confirmed by cycloheximide chase analysis of protein degradation.

In contrast, the PXR agonist rifampicin, strongly (7-fold) induced PXR-dependent transactivation of CYP3A4 promotor (Fig. 12). In antagonistic mode (LS180 cells were treated with RIF and GO at the same time) a decrease in PXR-dependent transactivation of *CYP3A4* promotor was observed (Fig. 13). Similarly, the exposure of LS180 cell line to graphene oxide led to dose-dependent and statistically significant decrease in RIF-induced *CYP3A4* and *MDR1* gene expressions (Fig. 14, Fig. 15). When

comparing the effect of GO on RIF-induced *MDR1* and RIF-induced *CYP3A4* gene expression, the decrease in the *MDR1* gene expression was more intense, nevertheless the trend was the same in both cases. At the protein level, no change or small increment in RIF-dependent CYP3A4 protein level was noticed (except medium-size particles, where CYP3A4 protein level dropped) after GO+RIF co-treatment (Fig. 16). In case of P-gp, the RIF-induced protein level was also elevated, further, with an increasing concentration of GO nanoparticles the RIF-induced P-gp level decreased dose-dependently (Fig. 17). Lammel *et al.* (2014) observed that cells co-treated with AhR agonist and GO, exhibited higher EROD activity than cells that were exposed to the AhR agonist alone, indicating that GO facilitates higher uptake of AhR agonists and leads to induction of *CYP1A* gene expression. In contrary, we observed moderate antagonistic activity of graphene oxide on the PXR signaling pathway at mRNA level when combined with PXR agonist rifampicin (Fig. 14, Fig. 15). Moreover, we observed that GO (0,2 and/or 2 μg/ml) caused the induction of RIF-dependent P-glycoprotein level, and that this induction declined with increasing concentration of GO nanoparticles (Fig. 17). Possible explanation of GO antagonistic activity could be in the higher degradation of PXR or proteins involved in transcription and translation. The stability and activity of PXR is regulated by post-translational modifications, such as phosphorylation or ubiquitination. Previously, an involvement of mTOR signaling pathway on PXR activity was observed (Ng *et al.*, 2011). Phosphorylation of PXR by p70S6 Kinase (substrate of mTOR) negatively regulates PXR transactivation function. It is known that mTOR kinase is essential in autophagy processes and GO was demonstrated to enhance genuine autophagy in the human-hamster hybrid (AL) cells at concentration 10 μg/ml (Liu *et al.*, 2016). This suggests that the GO could influence the PXR signaling pathway via mTOR intervention. Nevertheless, GO treatment did not influence the phosphorylation level of mTOR and its substrate p70S6 Kinase, which indicated that GO induced autophagy in a mTOR-independent manner (Liu *et al.*, 2016).

Higher production of ROS was also connected with higher levels of stress-activated-protein-kinases (SAPKs) (Benhar *et al.*, 2001, Chadee and Kyriakis, 2010). The activation of SAPK pathways might consequently lead to destabilization or degradation of pregnane X receptor. This work contributes to the knowledge about the effects of oxidezed graphene nanomaterials on PXR-related metabolism in humans.

However, the final effect of GO on LS180 cells and PXR signaling is a complex process of all points mentioned above, therefore further examinations are necessary.

6. Conclusion

1) Graphene oxide had moderate cytotoxic effect on the LS180 cell line, yet the reliability of MTT test might be compromised due to GO-MTT interactions.
2) Graphene oxide slightly induced the PXR activation at the highest concentration.
3) Graphene oxide itself did not influence the expression of PXR-driven genes, although when GO combined with PXR agonist, it caused slight dose-dependent decrease in *MDR1* gene expression.
4) Graphene oxide increased the level of PXR-regulated biotransformational enzymes, namely, CYP3A4 and P-glycoprotein, however when GO combined with PXR agonist, it caused dose-dependent decrease in RIF-induced P-glycoprotein level.
5) All together data indicated, that graphene oxide nanoparticles showed low cyto-toxicity towards the LS180 cell line, nevertheless they influenced the PXR signaling pathway, not only at the transcriptional level (antagonistic mode) but also on translational level (agonistic and antagonistic mode). The effect of graphene oxide nanoparticles was dose-dependent. Based on these results we conclude that GO NPs may cause drug-drug interactions and have an impact on human health.

7. Literature

Agarwal S., Zhou X., Ye F., He Q., Chen G. C., Soo J., Boey F., Zhang H. ,Chen P. (2010): Interfacing live cells with nanocarbon substrates. *Langmuir*, **26**, 2244-2247.

Akahoshi E., Yoshimura S. ,Ishihara-Sugano M. (2006): Over-expression of AhR (aryl hydrocarbon receptor) induces neural differentiation of Neuro2a cells: neurotoxicology study. *Environ Health*, **5**, 24.

Akhavan O. ,Ghaderi E. (2010): Toxicity of graphene and graphene oxide nanowalls against bacteria. *ACS Nano*, **4**, 5731-5736.

Akhavan O., Ghaderi E. ,Akhavan A. (2012): Size-dependent genotoxicity of graphene nanoplatelets in human stem cells. *Biomaterials*, **33**, 8017-8025.

Albermann N., Schmitz-Winnenthal F. H., Z'graggen K., Volk C., Hoffmann M. M., Haefeli W. E. ,Weiss J. (2005): Expression of the drug transporters MDR1/ABCB1, MRP1/ABCC1, MRP2/ABCC2, BCRP/ABCG2, and PXR in peripheral blood mononuclear cells and their relationship with the expression in intestine and liver. *Biochem Pharmacol*, **70**, 949-958.

Ambudkar S. V., Dey S., Hrycyna C. A., Ramachandra M., Pastan I. ,Gottesman M. M. (1999): Biochemical, cellular, and pharmacological aspects of the multidrug transporter. *Annu Rev Pharmacol Toxicol*, **39**, 361-398.

Anzenbacher P. ,Anzenbacherova E. (2001): Cytochromes P450 and metabolism of xenobiotics. *Cell Mol Life Sci*, **58**, 737-747.

Artiles M. S., Rout C. S. ,Fisher T. S. (2011): Graphene-based hybrid materials and devices for biosensing. *Adv Drug Deliv Rev*, **63**, 1352-1360.

Bao H., Pan Y., Ping Y., Sahoo N. G., Wu T., Li L., Li J. ,Gan L. H. (2011): Chitosan-functionalized graphene oxide as a nanocarrier for drug and gene delivery. *Small*, **7**, 1569-1578.

Benhar M., Dalyot I., Engelberg D. ,Levitzki A. (2001): Enhanced ROS production in oncogenically transformed cells potentiates c-Jun N-terminal kinase and p38 mitogen-activated protein kinase activation and sensitization to genotoxic stress. *Mol Cell Biol*, **21**, 6913-6926.

Bernhardt R. (2006): Cytochromes P450 as versatile biocatalysts. *J Biotechnol*, **124**, 128-145.

Bertilsson G., Heidrich J., Svensson K., Asman M., Jendeberg L., Sydow-Backman M., Ohlsson R., Postlind H., Blomquist P. ,Berkenstam A. (1998): Identification of a human nuclear receptor defines a new signaling pathway for CYP3A induction. *Proc Natl Acad Sci U S A*, **95**, 12208-12213.

Boitano A. E., Wang J., Romeo R., Bouchez L. C., Parker A. E., Sutton S. E., Walker J. R., Flaveny C. A., Perdew G. H., Denison M. S., Schultz P. G. ,Cooke M. P. (2010): Aryl hydrocarbon receptor antagonists promote the expansion of human hematopoietic stem cells. *Science*, **329**, 1345-1348.

Brigger I., Dubernet C. ,Couvreur P. (2002): Nanoparticles in cancer therapy and diagnosis. *Adv Drug Deliv Rev*, **54**, 631-651.

Cordon-Cardo C., O'brien J. P., Boccia J., Casals D., Bertino J. R. ,Melamed M. R. (1990): Expression of the multidrug resistance gene product (P-glycoprotein) in human normal and tumor tissues. *J Histochem Cytochem*, **38**, 1277-1287.

Creighton M. A., Rangel-Mendez J. R., Huang J., Kane A. B. ,Hurt R. H. (2013): Graphene-Induced Adsorptive and Optical Artifacts During In Vitro Toxicology Assays. *Small*, **9**, 1921-1927.

Cui Z., Han S. J., Vangasseri D. P. ,Huang L. (2005): Immunostimulation mechanism of LPD nanoparticle as a vaccine carrier. *Mol Pharm*, **2**, 22-28.

Daly A. K. (2006): Significance of the minor cytochrome P450 3A isoforms. *Clin Pharmacokinet*, **45**, 13-31.

Ding X. ,Kaminsky L. S. (2003): Human extrahepatic cytochromes P450: function in xenobiotic metabolism and tissue-selective chemical toxicity in the respiratory and gastrointestinal tracts. *Annu Rev Pharmacol Toxicol*, **43**, 149-173.

Dobson J. (2001): Nanoscale biogenic iron oxides and neurodegenerative disease. *FEBS Lett*, **496**, 1-5.

Dusso A. S., Brown A. J. ,Slatopolsky E. (2005): Vitamin D. *Am J Physiol Renal Physiol*, **289**, F8-28.

Elbi C., Misteli T. ,Hager G. L. (2002): Recruitment of dioxin receptor to active transcription sites. *Mol Biol Cell*, **13**, 2001-2015.

Emtsev K. V., Bostwick A., Horn K., Jobst J., Kellogg G. L., Ley L., Mcchesney J. L., Ohta T., Reshanov S. A., Rohrl J., Rotenberg E., Schmid A. K., Waldmann D., Weber H. B. ,Seyller T. (2009): Towards wafer-size graphene layers by atmospheric pressure graphitization of silicon carbide. *Nat Mater*, **8**, 203-207.

Enoki T. ,Takai K. (2008): Unconventional electronic and magnetic functions of nanographene-based host-guest systems. *Dalton Trans*, 3773-3781.

Feng L., Zhang S. ,Liu Z. (2011): Graphene based gene transfection. *Nanoscale*, **3**, 1252-1257.

Fromm M. F. (2004): Importance of P-glycoprotein at blood-tissue barriers. *Trends Pharmacol Sci*, **25**, 423-429.

Ferenčík, M., Škárka, B., Novák, M., Turecký, B. (2000): *Biochémia,* Alfa, Bratislava, 924 s., ISBN 80-88968-18-2.

Gao W., Alemany L. B., Ci L. ,Ajayan P. M. (2009): New insights into the structure and reduction of graphite oxide. *Nat Chem*, **1**, 403-408.

Gao X., Chan W. C. ,Nie S. (2002): Quantum-dot nanocrystals for ultrasensitive biological labeling and multicolor optical encoding. *J Biomed Opt*, **7**, 532-537.

Gasiewicz T. A., Singh K. P. ,Casado F. L. (2010): The aryl hydrocarbon receptor has an important role in the regulation of hematopoiesis: implications for benzene-induced hematopoietic toxicity. *Chem Biol Interact*, **184**, 246-251.

Geick A., Eichelbaum M. ,Burk O. (2001): Nuclear receptor response elements mediate induction of intestinal MDR1 by rifampin. *J Biol Chem*, **276**, 14581-14587.

Geim A. K. ,Novoselov K. S. (2007): The rise of graphene. *Nat Mater*, **6**, 183-191.

Geiser M., Rothen-Rutishauser B., Kapp N., Schurch S., Kreyling W., Schulz H., Semmler M., Im Hof V., Heyder J. ,Gehr P. (2005): Ultrafine particles cross cellular membranes by nonphagocytic mechanisms in lungs and in cultured cells. *Environ Health Perspect*, **113**, 1555-1560.

Glatt H., Boeing H., Engelke C. E., Ma L., Kuhlow A., Pabel U., Pomplun D., Teubner W. ,Meinl W. (2001): Human cytosolic sulphotransferases: genetics, characteristics, toxicological aspects. *Mutat Res*, **482**, 27-40.

Goodwin B. ,Moore J. T. (2004): CAR: detailing new models. *Trends Pharmacol Sci*, **25**, 437-441.

Gottesman M. M. ,Pastan I. (1993): Biochemistry of multidrug resistance mediated by the multidrug transporter. *Annu Rev Biochem*, **62**, 385-427.

Graham-Lorence S., Truan G., Peterson J. A., Falck J. R., Wei S., Helvig C. ,Capdevila J. H. (1997): An active site substitution, F87V, converts cytochrome P450 BM-3 into a regio- and stereoselective (14S,15R)-arachidonic acid epoxygenase. *J Biol Chem*, **272**, 1127-1135.

Greiner B., Eichelbaum M., Fritz P., Kreichgauer H. P., Von Richter O., Zundler J. ,Kroemer H. K. (1999): The role of intestinal P-glycoprotein in the interaction of digoxin and rifampin. *J Clin Invest*, **104**, 147-153.

Haehner B. D., Gorski J. C., Vandenbranden M., Wrighton S. A., Janardan S. K., Watkins P. B. ,Hall S. D. (1996): Bimodal distribution of renal cytochrome P450 3A activity in humans. *Mol Pharmacol*, **50**, 52-59.

Heersche H. B., Jarillo-Herrero P., Oostinga J. B., Vandersypen L. M. ,Morpurgo A. F. (2007): Bipolar supercurrent in graphene. *Nature*, **446**, 56-59.

Hendrychova T., Anzenbacherova E., Hudecek J., Skopalik J., Lange R., Hildebrandt P., Otyepka M. ,Anzenbacher P. (2011): Flexibility of human cytochrome P450 enzymes: molecular dynamics and spectroscopy reveal important function-related variations. *Biochim Biophys Acta*, **1814**, 58-68.

Hodgson E. (2012): Metabolic interactions of environmental toxicants in humans. *Prog Mol Biol Transl Sci*, **112**, 349-372.

Hu G., Xu C. ,Staudinger J. L. (2010a): Pregnane X receptor is SUMOylated to repress the inflammatory response. *J Pharmacol Exp Ther*, **335**, 342-350.

Hu W., Peng C., Luo W., Lv M., Li X., Li D., Huang Q. ,Fan C. (2010b): Graphene-based antibacterial paper. *ACS Nano*, **4**, 4317-4323.

Huang J., Zong C., Shen H., Liu M., Chen B., Ren B. ,Zhang Z. (2012): Mechanism of cellular uptake of graphene oxide studied by surface-enhanced Raman spectroscopy. *Small*, **8**, 2577-2584.

Chadee D. N. ,Kyriakis J. M. (2010): Activation of SAPK/JNKs in vitro. *Methods Mol Biol*, **661**, 59-73.

Chang Y., Yang S. T., Liu J. H., Dong E., Wang Y., Cao A., Liu Y. ,Wang H. (2011): In vitro toxicity evaluation of graphene oxide on A549 cells. *Toxicol Lett*, **200**, 201-210.

Jaiswal J. K., Goldman E. R., Mattoussi H. ,Simon S. M. (2004): Use of quantum dots for live cell imaging. *Nat Methods*, **1**, 73-78.

Jaiswal J. K., Mattoussi H., Mauro J. M. ,Simon S. M. (2003): Long-term multiple color imaging of live cells using quantum dot bioconjugates. *Nat Biotechnol*, **21**, 47-51.

Jancova P., Anzenbacher P. ,Anzenbacherova E. (2010): Phase II drug metabolizing enzymes. *Biomed Pap Med Fac Univ Palacky Olomouc Czech Repub*, **154**, 103-116.

Jiao G., He X., Li X., Qiu J., Xu H., Zhang N., Liu S. (2015): Limitations of MTT and CCK-8 assay for evaluation of graphene cytotoxicity. *RSC Advances*, **5**, 53240-53244.

Juliano R. L. ,Ling V. (1976): A surface glycoprotein modulating drug permeability in Chinese hamster ovary cell mutants. *Biochim Biophys Acta,* **455**, 152-162.

Karamani A. A., Douvalis A. P. ,Stalikas C. D. (2013): Zero-valent iron/iron oxide-oxyhydroxide/graphene as a magnetic sorbent for the enrichment of polychlorinated biphenyls, polyaromatic hydrocarbons and phthalates prior to gas chromatography-mass spectrometry. *J Chromatogr A,* **1271**, 1-9.

Kewley R. J., Whitelaw M. L. ,Chapman-Smith A. (2004): The mammalian basic helix-loop-helix/PAS family of transcriptional regulators. *Int J Biochem Cell Biol,* **36**, 189-204.

Kim J. S., Yoon T. J., Yu K. N., Kim B. G., Park S. J., Kim H. W., Lee K. H., Park S. B., Lee J. K. ,Cho M. H. (2006): Toxicity and tissue distribution of magnetic nanoparticles in mice. *Toxicol Sci,* **89**, 338-347.

King C. D., Rios G. R., Green M. D. ,Tephly T. R. (2000): UDP-glucuronosyltransferases. *Curr Drug Metab,* **1**, 143-161.

Kiss E. A., Vonarbourg C., Kopfmann S., Hobeika E., Finke D., Esser C. ,Diefenbach A. (2011): Natural aryl hydrocarbon receptor ligands control organogenesis of intestinal lymphoid follicles. *Science,* **334**, 1561-1565.

Klaine S. J., Alvarez P. J., Batley G. E., Fernandes T. F., Handy R. D., Lyon D. Y., Mahendra S., Mclaughlin M. J. ,Lead J. R. (2008): Nanomaterials in the environment: behavior, fate, bioavailability, and effects. *Environ Toxicol Chem,* **27**, 1825-1851.

Kliewer S. A., Moore J. T., Wade L., Staudinger J. L., Watson M. A., Jones S. A., Mckee D. D., Oliver B. B., Willson T. M., Zetterstrom R. H., Perlmann T. ,Lehmann J. M. (1998): An orphan nuclear receptor activated by pregnanes defines a novel steroid signaling pathway. *Cell,* **92**, 73-82.

Kliewer S. A. ,Willson T. M. (2002): Regulation of xenobiotic and bile acid metabolism by the nuclear pregnane X receptor. *J Lipid Res,* **43**, 359-364.

Kodama S. ,Negishi M. (2013): PXR cross-talks with internal and external signals in physiological and pathophysiological responses. *Drug Metab Rev,* **45**, 300-310.

Kuila T., Bose S., Khanra P., Mishra A. K., Kim N. H. ,Lee J. H. (2011): Recent advances in graphene-based biosensors. *Biosens Bioelectron,* **26**, 4637-4648.

Kuilla T., Bhadra S., Yao D., Kim NH., Bose S., Lee JH. (2010): Recent advances in graphene based polymer composites. *Progress in Polymer Science,* **35**, 1350-1375.

La W. G., Jin M., Park S., Yoon H. H., Jeong G. J., Bhang S. H., Park H., Char K. ,Kim B. S. (2014): Delivery of bone morphogenetic protein-2 and substance P using graphene oxide for bone regeneration. *Int J Nanomedicine,* **9 Suppl 1**, 107-116.

Lammel T., Boisseaux P., Fernandez-Cruz M. L. ,Navas J. M. (2013): Internalization and cytotoxicity of graphene oxide and carboxyl graphene nanoplatelets in the human hepatocellular carcinoma cell line Hep G2. *Part Fibre Toxicol,* **10**, 27.

Lammel T. ,Navas J. M. (2014): Graphene nanoplatelets spontaneously translocate into the cytosol and physically interact with cellular organelles in the fish cell line PLHC-1. *Aquat Toxicol,* **150**, 55-65.

Lead J. R., De Momi A., Goula G. ,Baker A. (2006): Fractionation of freshwater colloids and particles by SPLITT: analysis by electron microscopy and 3D excitation-emission matrix fluorescence. *Anal Chem,* **78**, 3609-3615.

Lee C., Wei X., Kysar J. W. ,Hone J. (2008): Measurement of the elastic properties and intrinsic strength of monolayer graphene. *Science,* **321**, 385-388.

Lee W. C., Lim C. H., Shi H., Tang L. A., Wang Y., Lim C. T. ,Loh K. P. (2011): Origin of enhanced stem cell growth and differentiation on graphene and graphene oxide. *ACS Nano,* **5**, 7334-7341.

Lehmann J. M., Mckee D. D., Watson M. A., Willson T. M., Moore J. T. ,Kliewer S. A. (1998): The human orphan nuclear receptor PXR is activated by compounds that regulate CYP3A4 gene expression and cause drug interactions. *J Clin Invest,* **102**, 1016-1023.

Li Y., Innocentin S., Withers D. R., Roberts N. A., Gallagher A. R., Grigorieva E. F., Wilhelm C. ,Veldhoen M. (2011): Exogenous stimuli maintain intraepithelial lymphocytes via aryl hydrocarbon receptor activation. *Cell,* **147**, 629-640.

Li Y., Liu Y., Fu Y., Wei T., Le Guyader L., Gao G., Liu R. S., Chang Y. Z. ,Chen C. (2012): The triggering of apoptosis in macrophages by pristine graphene through the MAPK and TGF-beta signaling pathways. *Biomaterials,* **33**, 402-411.

Liao KH., Lin YS., Macosko Ch. W., Haynes Ch. L. (2011): Cytotoxicity of Graphene Oxide and Graphene in Human Erythricytes and Skin Fibroblasts. *Applied materials and interfaces,* **3**, 2607-2615.

Lichti-Kaiser K., Brobst D., Xu C. ,Staudinger J. L. (2009a): A systematic analysis of predicted phosphorylation sites within the human pregnane X receptor protein. *J Pharmacol Exp Ther*, **331**, 65-76.

Lichti-Kaiser K., Xu C. ,Staudinger J. L. (2009b): Cyclic AMP-dependent protein kinase signaling modulates pregnane x receptor activity in a species-specific manner. *J Biol Chem*, **284**, 6639-6649.

Lindsey S. ,Papoutsakis E. T. (2011): The aryl hydrocarbon receptor (AHR) transcription factor regulates megakaryocytic polyploidization. *Br J Haematol*, **152**, 469-484.

Liu Y., Wang X., Wang J., Nie Y., Du H., Dai H., Wang J., Wang M., Chen S., Hei T. K., Deng Z., Wu L. ,Xu A. (2016): Graphene Oxide Attenuates the Cytotoxicity and Mutagenicity of PCB 52 via Activation of Genuine Autophagy. *Environ Sci Technol*, **50**, 3154-3164.

Liu Z., Robinson J. T., Sun X. ,Dai H. (2008): PEGylated nanographene oxide for delivery of water-insoluble cancer drugs. *J Am Chem Soc*, **130**, 10876-10877.

Maglich J. M., Stoltz C. M., Goodwin B., Hawkins-Brown D., Moore J. T. ,Kliewer S. A. (2002): Nuclear pregnane x receptor and constitutive androstane receptor regulate overlapping but distinct sets of genes involved in xenobiotic detoxification. *Mol Pharmacol*, **62**, 638-646.

Mangelsdorf D. J., Thummel C., Beato M., Herrlich P., Schutz G., Umesono K., Blumberg B., Kastner P., Mark M., Chambon P. ,Evans R. M. (1995): The nuclear receptor superfamily: the second decade. *Cell*, **83**, 835-839.

Massey V. (1994): Activation of molecular oxygen by flavins and flavoproteins. *J Biol Chem*, **269**, 22459-22462.

Medintz I. L., Uyeda H. T., Goldman E. R. ,Mattoussi H. (2005): Quantum dot bioconjugates for imaging, labelling and sensing. *Nat Mater*, **4**, 435-446.

Mimura J., Ema M., Sogawa K. ,Fujii-Kuriyama Y. (1999): Identification of a novel mechanism of regulation of Ah (dioxin) receptor function. *Genes Dev*, **13**, 20-25.

Moreau A., Vilarem M. J., Maurel P. ,Pascussi J. M. (2008): Xenoreceptors CAR and PXR activation and consequences on lipid metabolism, glucose homeostasis, and inflammatory response. *Mol Pharm*, **5**, 35-41.

Na H. K., Kim M. H., Lee J., Kim Y. K., Jang H., Lee K. E., Park H., Heo W. D., Jeon H., Choi I. S., Lee Y. ,Min D. H. (2013): Cytoprotective effects of graphene oxide for mammalian cells against internalization of exogenous materials. *Nanoscale*, **5**, 1669-1677.

Nakada K., Fujita M., Dresselhaus G. ,Dresselhaus M. S. (1996): Edge state in graphene ribbons: Nanometer size effect and edge shape dependence. *Phys Rev B Condens Matter*, **54**, 17954-17961.

Nakamura K., Moore R., Negishi M. ,Sueyoshi T. (2007): Nuclear pregnane X receptor cross-talk with FoxA2 to mediate drug-induced regulation of lipid metabolism in fasting mouse liver. *J Biol Chem*, **282**, 9768-9776.

Nakata K., Tanaka Y., Nakano T., Adachi T., Tanaka H., Kaminuma T. ,Ishikawa T. (2006): Nuclear receptor-mediated transcriptional regulation in Phase I, II, and III xenobiotic metabolizing systems. *Drug Metab Pharmacokinet*, **21**, 437-457.

Nasrollahzadeh M., Babaei F., Fakhri P., Jaleh B. (2015): Synthesis, characterization, structural, optical properties and catalytic activity of reduced graphene oxide/copper nanocomposites. *RSC Advances*, **5**, 107782-10789.

Nayak T. R., Andersen H., Makam V. S., Khaw C., Bae S., Xu X., Ee P. L., Ahn J. H., Hong B. H., Pastorin G. ,Ozyilmaz B. (2011): Graphene for controlled and accelerated osteogenic differentiation of human mesenchymal stem cells. *ACS Nano*, **5**, 4670-4678.

Nebert D. W. ,Nelson D. R. (1991): P450 gene nomenclature based on evolution. *Methods Enzymol*, **206**, 3-11.

Nelson D. R., Kamataki T., Waxman D. J., Guengerich F. P., Estabrook R. W., Feyereisen R., Gonzalez F. J., Coon M. J., Gunsalus I. C., Gotoh O. ,Et Al. (1993): The P450 superfamily: update on new sequences, gene mapping, accession numbers, early trivial names of enzymes, and nomenclature. *DNA Cell Biol*, **12**, 1-51.

Nelson D. R., Zeldin D. C., Hoffman S. M., Maltais L. J., Wain H. M. ,Nebert D. W. (2004): Comparison of cytochrome P450 (CYP) genes from the mouse and human genomes, including nomenclature recommendations for genes, pseudogenes and alternative-splice variants. *Pharmacogenetics*, **14**, 1-18.

Ng, D., Tie, S., Ong, P., Lim, W., Muhammad, T., Choo, Q., Chew, C. (2011): Rapamycin pretreatment abrogates Tumor Necrosis Factor-alpha donw-regulatory effects on LXRalpha and PXR mRNA expression via inhibition of c-Jun N-terminal kinase 1 activation in HepG2 cells. *Electronic Journal of Biotechnology*, **14**, 9-15.

Novoselov K. S., Jiang Z., Zhang Y., Morozov S. V., Stormer H. L., Zeitler U., Maan J. C., Boebinger G. S., Kim P. ,Geim A. K. (2007): Room-temperature quantum Hall effect in graphene. *Science*, **315**, 1379.

Olefsky J. M. (2001): Nuclear receptor minireview series. *J Biol Chem*, **276**, 36863-36864.

Omura T. ,Sato R. (1964): The Carbon Monoxide-Binding Pigment of Liver Microsomes. I. Evidence for Its Hemoprotein Nature. *J Biol Chem*, **239**, 2370-2378.

Pan B. F., Dutt A. ,Nelson J. A. (1994): Enhanced transepithelial flux of cimetidine by Madin-Darby canine kidney cells overexpressing human P-glycoprotein. *J Pharmacol Exp Ther*, **270**, 1-7.

Panyam J. ,Labhasetwar V. (2003): Biodegradable nanoparticles for drug and gene delivery to cells and tissue. *Adv Drug Deliv Rev*, **55**, 329-347.

Park S. ,Ruoff R. S. (2009): Chemical methods for the production of graphenes. *Nat Nanotechnol*, **4**, 217-224.

Pasquel D., Doricakova A., Li H., Kortagere S., Krasowski M. D., Biswas A., Walton W. G., Redinbo M. R., Dvorak Z. ,Mani S. (2016): Acetylation of lysine 109 modulates pregnane X receptor DNA binding and transcriptional activity. *Biochim Biophys Acta*, **1859**, 1155-1169.

Pavek P., Pospechova K., Svecova L., Syrova Z., Stejskalova L., Blazkova J., Dvorak Z. ,Blahos J. (2010): Intestinal cell-specific vitamin D receptor (VDR)-mediated transcriptional regulation of CYP3A4 gene. *Biochem Pharmacol*, **79**, 277-287.

Pelkonen O., Maenpaa J., Taavitsainen P., Rautio A. ,Raunio H. (1998): Inhibition and induction of human cytochrome P450 (CYP) enzymes. *Xenobiotica*, **28**, 1203-1253.

Pondugula S. R., Dong H. ,Chen T. (2009): Phosphorylation and protein-protein interactions in PXR-mediated CYP3A repression. *Expert Opin Drug Metab Toxicol*, **5**, 861-873.

Pospechova K., Rozehnal V., Stejskalova L., Vrzal R., Pospisilova N., Jamborova G., May K., Siegmund W., Dvorak Z., Nachtigal P., Semecky V. ,Pavek P. (2009): Expression and activity of vitamin D receptor in the human placenta and in choriocarcinoma BeWo and JEG-3 cell lines. *Mol Cell Endocrinol*, **299**, 178-187.

Pulskamp K., Diabate S. ,Krug H. F. (2007): Carbon nanotubes show no sign of acute toxicity but induce intracellular reactive oxygen species in dependence on contaminants. *Toxicol Lett*, **168**, 58-74.

Quintana F. J., Basso A. S., Iglesias A. H., Korn T., Farez M. F., Bettelli E., Caccamo M., Oukka M. ,Weiner H. L. (2008): Control of T(reg) and T(H)17 cell differentiation by the aryl hydrocarbon receptor. *Nature*, **453**, 65-71.

Ritter K. A. ,Lyding J. W. (2009): The influence of edge structure on the electronic properties of graphene quantum dots and nanoribbons. *Nat Mater*, **8**, 235-242.

Roduner E. (2006): Size matters: why nanomaterials are different. *Chem Soc Rev*, **35**, 583-592.

Rysa J., Buler M., Savolainen M. J., Ruskoaho H., Hakkola J. ,Hukkanen J. (2013): Pregnane X receptor agonists impair postprandial glucose tolerance. *Clin Pharmacol Ther*, **93**, 556-563.

Sanchez V. C., Jachak A., Hurt R. H. ,Kane A. B. (2012): Biological interactions of graphene-family nanomaterials: an interdisciplinary review. *Chem Res Toxicol*, **25**, 15-34.

Sasidharan A., Panchakarla L. S., Chandran P., Menon D., Nair S., Rao C. N. ,Koyakutty M. (2011): Differential nano-bio interactions and toxicity effects of pristine versus functionalized graphene. *Nanoscale*, **3**, 2461-2464.

Sasidharan A., Panchakarla L. S., Sadanandan A. R., Ashokan A., Chandran P., Girish C. M., Menon D., Nair S. V., Rao C. N. ,Koyakutty M. (2012): Hemocompatibility and macrophage response of pristine and functionalized graphene. *Small*, **8**, 1251-1263.

Scott E. E. ,Halpert J. R. (2005): Structures of cytochrome P450 3A4. *Trends Biochem Sci*, **30**, 5-7.

Sharom F. J. (2014): Complex Interplay between the P-Glycoprotein Multidrug Efflux Pump and the Membrane: Its Role in Modulating Protein Function. *Front Oncol*, **4**, 41.

Sheehan D., Meade G., Foley V. M. ,Dowd C. A. (2001): Structure, function and evolution of glutathione transferases: implications for classification of non-mammalian members of an ancient enzyme superfamily. *Biochem J*, **360**, 1-16.

Shen J., Zhu Y., Yang X. ,Li C. (2012): Graphene quantum dots: emergent nanolights for bioimaging, sensors, catalysis and photovoltaic devices. *Chem Commun (Camb)*, **48**, 3686-3699.

Shvedova A. A., Pietroiusti A., Fadeel B. ,Kagan V. E. (2012): Mechanisms of carbon nanotube-induced toxicity: focus on oxidative stress. *Toxicol Appl Pharmacol*, **261**, 121-133.

Schinkel A. H. (1997): The physiological function of drug-transporting P-glycoproteins. *Semin Cancer Biol*, **8**, 161-170.

Schinkel A. H. ,Jonker J. W. (2003): Mammalian drug efflux transporters of the ATP binding cassette (ABC) family: an overview. *Adv Drug Deliv Rev*, **55**, 3-29.

Skálová, L., Boušová, I., Machala, M., Pávek, P., Podlipná, R., Souček, P., Szotáková, B., Vondráček, J., Wsól, V., (2011): *Metabolismus léčiv a jiných xenobiotik.*1. vyd. Praha: Karolinum, 978-80-246-1917-0.

Smith D. A. ,Jones B. C. (1992): Speculations on the substrate structure-activity relationship (SSAR) of cytochrome P450 enzymes. *Biochem Pharmacol,* **44**, 2089-2098.

Smutny T., Bitman M., Urban M., Dubecka M., Vrzal R., Dvorak Z. ,Pavek P. (2014): U0126, a mitogen-activated protein kinase kinase 1 and 2 (MEK1 and 2) inhibitor, selectively up-regulates main isoforms of CYP3A subfamily via a pregnane X receptor (PXR) in HepG2 cells. *Arch Toxicol,* **88**, 2243-2259.

Smutny T., Mani S. ,Pavek P. (2013): Post-translational and post-transcriptional modifications of pregnane X receptor (PXR) in regulation of the cytochrome P450 superfamily. *Curr Drug Metab,* **14**, 1059-1069.

Staudinger J., Liu Y., Madan A., Habeebu S. ,Klaassen C. D. (2001): Coordinate regulation of xenobiotic and bile acid homeostasis by pregnane X receptor. *Drug Metab Dispos,* **29**, 1467-1472.

Staudinger J. L., Xu C., Biswas A. ,Mani S. (2011): Post-translational modification of pregnane x receptor. *Pharmacol Res,* **64**, 4-10.

Svecova L., Vrzal R., Burysek L., Anzenbacherova E., Cerveny L., Grim J., Trejtnar F., Kunes J., Pour M., Staud F., Anzenbacher P., Dvorak Z. ,Pavek P. (2008): Azole antimycotics differentially affect rifampicin-induced pregnane X receptor-mediated CYP3A4 gene expression. *Drug Metab Dispos,* **36**, 339-348.

Synold T. W., Dussault I. ,Forman B. M. (2001): The orphan nuclear receptor SXR coordinately regulates drug metabolism and efflux. *Nat Med,* **7**, 584-590.

Tan H., Xu C., Zeng H., Wang Y., Li Y., Fan X., Chen P., Jiang Y., Chen X., Huang M. ,Bi H. (2016): SUMOylation of pregnane X receptor suppresses rifampicin-induced CYP3A4 and P-gp expression and activity in LS174T cells. *J Pharmacol Sci,* **130**, 66-71.

Thiebaut F., Tsuruo T., Hamada H., Gottesman M. M., Pastan I. ,Willingham M. C. (1987): Cellular localization of the multidrug-resistance gene product P-glycoprotein in normal human tissues. *Proc Natl Acad Sci U S A,* **84**, 7735-7738.

Tian Y. (2013): Epigenetic regulation of pregnane X receptor activity. *Drug Metab Rev,* **45**, 166-172.

Tirona R. G. ,Kim R. B. (2005): Nuclear receptors and drug disposition gene regulation. *J Pharm Sci,* **94**, 1169-1186.

Tirona R. G., Lee W., Leake B. F., Lan L. B., Cline C. B., Lamba V., Parviz F., Duncan S. A., Inoue Y., Gonzalez F. J., Schuetz E. G. ,Kim R. B. (2003): The orphan nuclear receptor HNF4alpha determines PXR- and CAR-mediated xenobiotic induction of CYP3A4. *Nat Med,* **9**, 220-224.

Tkachev S. V., Buslaeva E. Yu., Gubin S. P. (2011): Graphene : A novel carbon nanomaterial. *Inorganic materials,* **47,** 1-10.

Tsai Y. C. ,Huang J. D. (2007): Multiwalled carbon nanotube-poly(vinyl alcohol)-glucose oxidase nanobiocomposites for amperometric sensing. *J Nanosci Nanotechnol,* **7**, 3227-3232.

Tsai Y. C., Huang J. D. ,Chiu C. C. (2007): Amperometric ethanol biosensor based on poly(vinyl alcohol)-multiwalled carbon nanotube-alcohol dehydrogenase biocomposite. *Biosens Bioelectron,* **22**, 3051-3056.

Ueda A., Hamadeh H. K., Webb H. K., Yamamoto Y., Sueyoshi T., Afshari C. A., Lehmann J. M. ,Negishi M. (2002): Diverse roles of the nuclear orphan receptor CAR in regulating hepatic genes in response to phenobarbital. *Mol Pharmacol,* **61**, 1-6.

Ueda K., Taguchi Y. ,Morishima M. (1997): How does P-glycoprotein recognize its substrates? *Semin Cancer Biol,* **8**, 151-159.

Vila M., Portoles M. T., Marques P. A., Feito M. J., Matesanz M. C., Ramirez-Santillan C., Goncalves G., Cruz S. M., Nieto A. ,Vallet-Regi M. (2012): Cell uptake survey of pegylated nanographene oxide. *Nanotechnology,* **23**, 465103.

Vrzal R., Ulrichova J. ,Dvorak Z. (2004): Aromatic hydrocarbon receptor status in the metabolism of xenobiotics under normal and pathophysiological conditions. *Biomed Pap Med Fac Univ Palacky Olomouc Czech Repub,* **148**, 3-10.

Walisser J. A., Glover E., Pande K., Liss A. L. ,Bradfield C. A. (2005): Aryl hydrocarbon receptor-dependent liver development and hepatotoxicity are mediated by different cell types. *Proc Natl Acad Sci U S A,* **102**, 17858-17863.

Wang K., Ruan J., Song H., Zhang J., Wo Y., Guo S. ,Cui D. (2011): Biocompatibility of Graphene Oxide. *Nanoscale Res Lett,* **6**, 8.

Watkins R. E., Wisely G. B., Moore L. B., Collins J. L., Lambert M. H., Williams S. P., Willson T. M., Kliewer S. A. ,Redinbo M. R. (2001): The human nuclear xenobiotic receptor PXR: structural determinants of directed promiscuity. *Science,* **292**, 2329-2333.

Westlind-Johnsson A., Malmebo S., Johansson A., Otter C., Andersson T. B., Johansson I., Edwards R. J., Boobis A. R. ,Ingelman-Sundberg M. (2003): Comparative analysis of CYP3A expression in human liver suggests only a minor role for CYP3A5 in drug metabolism. *Drug Metab Dispos,* **31**, 755-761.

Wienkers L. C. ,Heath T. G. (2005): Predicting in vivo drug interactions from in vitro drug discovery data. *Nat Rev Drug Discov,* **4**, 825-833.

Wrighton S. A., Vandenbranden M. ,Ring B. J. (1996): The human drug metabolizing cytochromes P450. *J Pharmacokinet Biopharm,* **24**, 461-473.

Wu C. Y., Benet L. Z., Hebert M. F., Gupta S. K., Rowland M., Gomez D. Y. ,Wacher V. J. (1995): Differentiation of absorption and first-pass gut and hepatic metabolism in humans: studies with cyclosporine. *Clin Pharmacol Ther,* **58**, 492-497.

Wu Z. S., Ren W., Gao L., Zhao J., Chen Z., Liu B., Tang D., Yu B., Jiang C. ,Cheng H. M. (2009): Synthesis of graphene sheets with high electrical conductivity and good thermal stability by hydrogen arc discharge exfoliation. *ACS Nano,* **3**, 411-417.

Xia T., Kovochich M., Brant J., Hotze M., Sempf J., Oberley T., Sioutas C., Yeh J. I., Wiesner M. R. ,Nel A. E. (2006): Comparison of the abilities of ambient and manufactured nanoparticles to induce cellular toxicity according to an oxidative stress paradigm. *Nano Lett,* **6**, 1794-1807.

Yang Y., Ren L., Zhang C., Huang S. ,Liu T. (2011): Facile fabrication of functionalized graphene sheets (FGS)/ZnO nanocomposites with photocatalytic property. *ACS Appl Mater Interfaces,* **3**, 2779-2785.

Yuan J., Gao H., Sui J., Duan H., Chen W. N. ,Ching C. B. (2012): Cytotoxicity evaluation of oxidized single-walled carbon nanotubes and graphene oxide on human hepatoma HepG2 cells: an iTRAQ-coupled 2D LC-MS/MS proteome analysis. *Toxicol Sci,* **126**, 149-161.

Yue H., Wei W., Yue Z., Wang B., Luo N., Gao Y., Ma D., Ma G. ,Su Z. (2012): The role of the lateral dimension of graphene oxide in the regulation of cellular responses. *Biomaterials,* **33**, 4013-4021.

Zhang L., Xing Y., He N., Zhang Y., Lu Z., Zhang J. ,Zhang Z. (2012): Preparation of graphene quantum dots for bioimaging application. *J Nanosci Nanotechnol,* **12**, 2924-2928.

Zhang Y., Ali S. F., Dervishi E., Xu Y., Li Z., Casciano D. ,Biris A. S. (2010): Cytotoxicity effects of graphene and single-wall carbon nanotubes in neural phaeochromocytoma-derived PC12 cells. *ACS Nano,* **4**, 3181-3186.

Zhi F., Dong H., Jia X., Guo W., Lu H., Yang Y., Ju H., Zhang X. ,Hu Y. (2013): Functionalized graphene oxide mediated adriamycin delivery and miR-21 gene silencing to overcome tumor multidrug resistance in vitro. *PLoS One,* **8**, e60034.

Zhou T., Zhou X. ,Xing D. (2014): Controlled release of doxorubicin from graphene oxide based charge-reversal nanocarrier. *Biomaterials,* **35**, 4185-4194.

Zhu J., Liao L., Bian X., Kong J., Yang P. ,Liu B. (2012): pH-controlled delivery of doxorubicin to cancer cells, based on small mesoporous carbon nanospheres. *Small,* **8**, 2715-2720.

Zhu S., Zhang J., Qiao C., Tang S., Li Y., Yuan W., Li B., Tian L., Liu F., Hu R., Gao H., Wei H., Zhang H., Sun H. ,Yang B. (2011): Strongly green-photoluminescent graphene quantum dots for bioimaging applications. *Chem Commun (Camb),* **47**, 6858-6860.